Formation and degradation of chaotic terrain in the Galaxias regions of Mars: implications for near-surface storage of ice

Journal Item

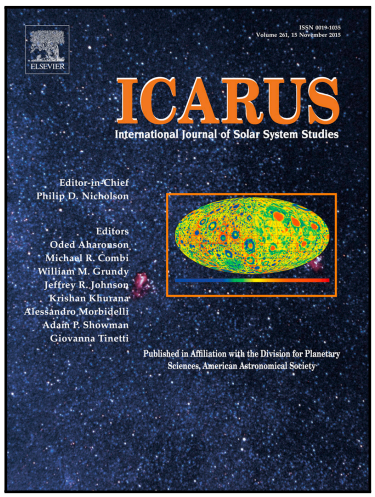

Formation and degradation of chaotic terrain in the Galaxias regions of Mars; implications for near-surface storage of ice

Colman Gallagher , Matt Balme , Richard Soare , Susan J. Conway

PII: S0019-1035(17)30588-2
DOI: 10.1016/j.icarus.2018.03.002
Reference: YICAR 12826

To appear in: *Icarus*

Received date: 11 August 2017
Revised date: 22 February 2018
Accepted date: 2 March 2018

Please cite this article as: Colman Gallagher , Matt Balme , Richard Soare , Susan J. Conway , Formation and degradation of chaotic terrain in the Galaxias regions of Mars; implications for near-surface storage of ice, *Icarus* (2018), doi: 10.1016/j.icarus.2018.03.002

Highlights

- A comprehensive integration of regional landforms and landscapes through observation and quantitative analyses.
- The landforms reflect the extensive loss of terrain through de-volatization of ice-rich surface units due to cryo-volcanic interactions.
- Resulted in 10^4 km^3 of ground-ice loss.
- Associated transmission of groundwater or low viscosity lava through underground conduits, leading to open-channel flow.
- Underscores the significance of cryo-volcanic interactions in the cycling of water between the Martian surface and the atmosphere.

Formation and degradation of chaotic terrain in the Galaxias regions of Mars; implications for near-surface storage of ice.

Colman Gallagher, UCD School of Geography, Belfield, Dublin 4, Ireland

UCD Earth Institute, Belfield, Dublin 4, Ireland

Matt Balme, Department of Physical Sciences, The Open University, Milton Keynes, UK

Richard Soare, Department of Geography, Dawson College, Montreal, Canada

Susan J. Conway, Laboratoire de Planétologie et Géodynamique de Nantes UMR-CNRS 6112, 2 rue de la Houssinière, BP 92208, 44322 NANTES Cedex 3, France

ABSTRACT

Galaxias Chaos is a region of low plateaus separated by narrow fractures – a chaotic terrain. Galaxias Mensae and Galaxias Colles are characterised by mesa and knobby terrains of individual landforms, or small assemblages, separated by plains. Galaxias Chaos has been attributed to ground disturbance due to sublimation in shallow subsurface ice-rich deposits, Galaxias Mensae and Galaxias Colles to sublimation and degradation of icy surface materials, without production of chaotic terrain. Liquid water has not been regarded as a product of the degradation of these icy terrains. This paper asks two research questions: (1) what was the total extent of the different modes of landscape degradation, especially chaotic terrain, involved in producing the present landscapes of Galaxias Chaos and Galaxias Mensae-Colles; (2) can the generation of liquid water as a product of landscape degradation be ruled-out? Using a morphological-statistical approach, including power spectrum analysis of relief, our observations and analyses show that present mesa-knobby terrains of Galaxias Mensae-Colles

evolved from a landscape that had the same directional pattern and relief as presently found in Galaxias Chaos. This terrain extended across ~440000 km^2 but ~22000 km^3 (average thickness, 77 m) have been lost across ~285000 km^2. This represents a significant loss of ice-bearing deposits. Moreover, this surface degradation was spatially partitioned by landforms associated with elevated ground heating and the transmission of a fluid in the shallow subsurface towards a distal channel. In answer to research question 2, it cannot be determined definitively if the fluid involved was groundwater, generated by the thermal destabilisation of the icy deposits, or low viscosity lava. However, it is likely that the degradation of Galaxias Mensae-Colles was not a consequence of sublimation alone. These findings underscore the significance of cryo-volcanic interactions in the cycling of water between the Martian surface and the atmosphere.

Key words: chaotic terrain; devolatization; ice loss; groundwater; landscape evolution; Mars.

1. INTRODUCTION

Galaxias Chaos (Carr and Schaber, 1977) and the adjoining regions Galaxias Mensae and Galaxias Colles (Fig. 1A, approximately 33° - 43° N, 144° - 156° E) are located at the topographic transition between the Elysium Rise and Utopia Planitia, with Phlegra Montes to the east (Fig. 1B). The distinctive chaotic terrain (Sharp, 1973) of Galaxias Chaos, blocky plateaus bounded by cross-cutting fracture-troughs (Fig. 2A), has been interpreted to be a consequence of ground disturbance due to sublimation and loss of volume in icy deposits underlying a surface lava cap (Pedersen and Head, 2011). The geomorphology of Galaxias Mensae and Galaxias Colles, dominated by mesas (Fig. 2B) and knobby terrain (Scott and Carr, 1978) (Fig. 2C), has been

explained as a consequence of sublimation from icy surface units but without the ground disturbance characteristic of chaotic terrain (Pedersen and Head, 2010).

The Galaxias regions (Galaxias Mensae is formally part of Galaxias Colles) are located close to Hecates Tholus, within the Elysium Volcanic Province (Platz and Michael, 2011), the second largest volcanic province on Mars (Fig. 1B). Elysium Mons became active 4 Ga (Hartmann and Berman, 2000) but plains lava flows from it were emplaced in Elysium Planitia within the last 10-100 Ma (Hartmann and Berman, 2000), perhaps as recently as 1-10 Ma (Vaucher et al., 2009). Volcanic eruptions from Hecates Tholus occurred until 335 Ma and the edifice was glaciated repeatedly and as recently as 0.1 Ma (Hauber et al., 2005; Pablo et al., 2013).

Neutron flux data (Boynton et al., 2002) indicate that the Galaxias regions are located at the margin of icy plains extending north from Elysium Mons and Hecates Tholus. These data indicate that surface layers poleward of ~45° N probably contain 1 – 2 wt% H_2O, increasing to 20 – 50 wt% H_2O from beyond several 10s of centimeters below the surface. Radar characterizations of icy deposits extending from ~38° - -48° N in western Utopia Planitia are consistent with the subsurface ice content reaching 50 – 85 vol% (Stuurman et al., 2016).

During the Early Amazonian Epoch, swarms of volcanic dikes were emplaced below these icy surface units (Pedersen et al., 2010), possibly including lowland glaciers (Mouginis-Mark and Wilson, 2016). Subsequently, disturbance, erosion and devolatization of the icy cover have exposed many of the dikes, the traces of which appear as parallel sets of linear fractures and

ridges striking SE-NW (Pedersen et al., 2010). In this context, Pedersen and Head (2010) concluded that the mesa terrain of Galaxias Mensae and knobby terrain of Galaxias Colles were formed through the sublimation and degradation of icy surface units without ground disturbance. By contrast Pedersen and Head (2011) interpreted the geomorphology of Galaxias Chaos to be a consequence of the disturbance of a lava cap in response to sublimation and loss of volume in underlying icy deposits. Significantly, neither interpretation involves the production of liquid water or the incision of channels as consequences of the devolatization. Rather, Hrad Vallis (Wilson and Mouginis-Mark, 2003; Hopper and Leverington, 2014) (Fig. 1B) and the channel extending NW from Galaxias Fossae (Fig. 1A and B, Fracture A) have been interpreted as having been incised either by mudflows, generated by interaction between volcanism and ice (De Hon, 1992; Wilson and Mouginis-Mark, 2003), or by low viscosity lavas (Hauber et al., 2005) that exploited structural features of Elysium Mons to reach the surrounding plains (Hopper and Leverington, 2014). However, elsewhere on Mars, significant groundwater and surface water discharges were associated with the formation of chaotic terrains due to ground disturbance associated with the drainage of aquifers that had been generated by the melting of ice in near surface deposits (Sharp, 1973; Carr, 1979). Therefore, determining the spatial extent of chaotic terrain production and, in particular, understanding the relationship between chaotic terrain and associated landforms indicative of specific devolatization mechanisms are important in identifying potential source-to-sink routeways and processes of water transfer in, and from, the Martian near-surface. For those reasons, and given the close relationship between ice and volcanism in the Galaxias regions, this paper asks two fundamental research questions: (1) what was the total extent of the different modes of landscape degradation, especially chaotic terrain

formation, involved in producing the present landscapes of Galaxias Chaos and Galaxias Mensae-Colles, and; (2) can the generation of liquid water as a product of regional landscape degradation be ruled-out?

2. DATA AND METHODS

2.1 Data

Landforms were mapped and measured from mosaiced CTX (ConTeXT imager, NASA Mars Reconnaissance Orbiter; Malin et al., 2007) visible-wavelength images (resolution ~6 m per pixel), displayed in a cylindrical projection (image credits: NASA/JPL-Caltech/MSSS). For synoptic coverage and small-scale mapping, THEMIS (Thermal Emission Imaging Spectrometer, NASA Odyssey; Christensen et al., 2004) daytime brightness records (credit: NASA/JPL-Caltech/Arizona State University) were also used. The CTX and THEMIS images were overlaid on the MOLA (Mars Orbiter Laser Altimeter; Smith et al., 2001) MEGDR (Mission Experiment Gridded Data Record. Credit: NASA/MOLA Science Team) digital terrain model (DTM), covering the entire study area at a resolution of ~463 m/pixel. Higher resolution elevation profiles of Galaxias Mensae and Galaxias Chaos were extracted from CTX images draped over a HRSC (High Resolution Stereo Camera; Neukum et al., 2004) DTM with a spatial resolution of 50 m per pixel and height accuracy of ~10 m per pixel (Jaumann et al., 2007; Gwinner et al., 2009) in a sinusoidal projection (image credits: ESA/DLR/FU Berlin). All imaging and elevation data were stored and manipulated in a Geographic Information System (GIS).

2.2 Methods

Broadly, the methodology was developed to test two fundamental hypotheses (*1H* and *2H*) via measurements providing a 3-dimensional quantification of the landscapes of the Galaxias regions. *1H* was that the extent of each Galaxias region can determined on the basis of identifying the spatial distributions of distinct regional landform assemblages, differentiated on the basis of quantifiably distinct directional arrangements. *1H* was tested by measuring the directional arrangement of landforms (*Section 2.2.1*) and using directional (circular) statistics to compare and contrast the directionality of the landforms within and between the regions (*Section 2.2.2*). The second fundamental hypothesis (*2H*) was that the relief of Galaxias Chaos is quantifiably distinct, in accord particularly with the morphological difference between its chaotic terrain and the mesa terrain of the neighbouring region of Galaxias Mensae. Validating *1H* and *2H* would support the interpretation of separate regional morphogeneses implied by the geomorphology. However, rejecting *1H* and *2H* would suggest a more complex evolutionary path leading to the present landscapes, and perhaps involving a common process if the regions are shown to have shared characteristics of relief.

The most obvious difference in geomorphology potentially contributing to regional variability in relief are the small (typically 10^{-1} km) horizontal separations between topographic highs in Galaxias Chaos, reflecting repeated plateau-trough-plateau oscillations in elevation, in contrast to the wide plains between topographic highs, the mesas, in Galaxias Mensae. Given these high-order variations in the horizontal separation of high and low terrain, the regions appear to be differentiated on the basis of the cyclicity of their relief, i.e. the horizontal scale over which their

relative relief oscillates from high to low. Accordingly, a power spectrum analysis (PSA) was used to test *2H* (*Section 2.2.3*). The PSA first determined if the chaotic terrain relief (Galaxias Chaos) and inter-mesa terrain relief (Galaxias Mensae) oscillate with statistically significant (i.e. non-random) cyclicities. If so, the PSA was then used to calculate the dominant horizontal scales over which the cyclicities of regional relief oscillates (L_{dom}). Statistical tests were then used to find if the dominant relief cyclicities of the chaotic terrain and inter-mesa terrain are significantly different from each other. Finding that the relief cyclicities of Galaxias Chaos and the inter-mesas of Galaxias Mensae are significantly different would support the interpretation that the regions are separate morphogenetic domains. Finding no significant difference in the relief cyclicity of the chaotic and inter-mesa terrains would prompt subsequent statistical testing to identify the factor underlying the shared cyclicity of relief (*Section 2.2.4*).

2.2.1 Measuring landform directional arrangement.

Measurements from the HRSC DTM and co-registered CTX images focused on the arrangement of mesa assemblages and inter-assemblage corridors (Fig. 3A - E) and the following features (Table 1): (1) the strike of fractures and lineaments; (2) the orientations of chaotic terrain plateaus and mesas, and; (3) the alignment of pitted cone chains and broad ridges. The orientations of plateau edges and mesa edges were digitised from the CTX images as straight line segments joined at vertices (Fig. 2A, B, C). To preclude projection-induced distortions, all directions were measured relative to true north and all distances, including along elevation profiles (e.g. Fig. 3A, B, C, D), were geodesic. The directional arrangements of mesa assemblages and inter-assemblage corridors in Galaxias Mensae (Fig. 3D) were determined by applying the

eight-direction pour-point (D-8) watershed analysis algorithm in the GIS to the HRSC DTM. Mesa assemblages were located by inverting the terrain in the DTM to find slope convergences occurring within a mutual elevation threshold, and with a specified minimum length, and then reinverting the DTM to plot these convergences correctly as ridges. The same analysis was applied, without terrain inversion, to locate and plot the axes of inter-assemblage corridors. The mesa assemblage ridges and inter-assemblage corridor axes were plotted as line segments joined at vertices and the bearing of each line segment was automatically measured in the GIS and plotted on a rose diagram (Fig. 3E). Fractures (Fig. 4), dark lineaments (Fig. 5), pitted cone chains (at least two cones in sequence) (Fig. 4B, C, D, F; Fig. 6; Fig. 7; Fig. 8) and broad ridges (Fig. 7) were digitised as straight line segments between vertices marking inflexions along the fractures and longitudinal axes of the landforms. In the statistical analysis of directional measurements, strikes, orientations and bearings were plotted on rose diagrams as axial planes (Fig. 3E and Fig. 9) and the statistical procedures took this into account when determining directional distributions and their associated probabilities against uniform distributions. All directional statistical analyses were performed using the PAleontological STatistics (PAST) V3.14 (Hammer et al., 2001; Hammer and Harper, 2006) software package.

	Galaxias Chaos	Galaxias Mensae	Galaxias Colles
Chaos plateau edge	•		
Mesa edge		•	•
Mesa assemblage/corridor		•	
Pitted cone chain/broad ridge	•	•	

Table 1. Feature classes used in the directional analysis.

2.2.2 Testing for non-uniform directional arrangement of landforms.

Testing for any correspondence between the directional arrangements of the landform features (Table 1) was a two-stage process. First, Rao's non-parametric U-Test (Hammer et al. 2001; Hammer and Harper, 2006) was used to determine if each feature has a statistically significant preferred directional distribution ($\alpha = 0.05$, against a uniform distribution). The Mardia-Watson-Wheeler B-Test (Hammer et al. 2001; Hammer and Harper, 2006) for equal distributions was then used to test H_0 pairwise between features found to have a statistically significant preferred directional distribution (Table 2). H_0 in these cases was that there is no significant difference ($\alpha = 0.05$) between the directional distributions of each pair of features. If H_0 cannot be rejected, each pair of landform features can be considered to have same directional distribution.

2.2.3 Cyclicity in the relief of Galaxias Chaos and the inter-mesas of Galaxias Mensae.

PSA was used to determine if there are statistically non-random cyclicities (i.e. a statistically significant repeating pattern of oscillating high and low elevations) in the relief of Galaxias Chaos and the inter-mesas of Galaxias Mensae. First, 15 elevation profiles were extracted from the HRSC DTM, with an overlay of CTX images, across Galaxias Chaos (Fig. 10A); the profiles were extracted along planes orthogonal to the strike of local primary fractures (~SE-NW). From the Galaxias Mensae inter-mesas, 23 elevation profiles were extracted, also orthogonal to local primary fractures (Fig. 10B). Elevations were measured at 50 m intervals in all profiles. PSA requires that the elevation (z) trend of each profile is removed. This was done by arithmetical degree 1 (d = 1) differencing (i.e. $z_{d1} = z_2 - z_1 \ldots z_{dn} = z_n - z_{n-1}$). Each resulting d = 1 elevation series is the first derivative of the parent elevation profile, describing the change in elevation with respect to distance along-profile, in multiples of the sampling interval of 50 m. The power spectral density of the d = 1 elevation series derived from the detrended chaotic terrain and inter-mesa terrain elevation profiles are shown as matrix plots (Fig. 11A and B), allowing simultaneous display of all power spectra from each region, rather than the conventional method of plotting the power spectra as individual periodograms. The matrix plots show the frequency peaks (and associated wavelengths, L) of each d = 1 elevation series and p(<0.05), the power level that must be exceeded for the statistical significance of frequency peaks in the spectra to exceed the critical probability level. Spectra that have no peaks exceeding p<0.05 are not significantly different from white noise and are considered random. The peak frequency (f_{peak}) of each power spectrum was automatically reported by the software and stored for analysis. Power is expressed as a non-dimensional multiple of unit average power (i.e. = 1). The

dominant wavelength (L_{dom}), i.e. the dominant horizontal scale over which relief oscillates, in each elevation profile was calculated from $L_{dom} = (1/lag)f_{peak}$, where the lag = 50 m (i.e. the along-profile sampling interval).

To test if the relief cyclicities of the chaotic and inter-mesa terrains are significantly different from each other, the non-parametric Mann-Whitney difference of medians U-Test was used (Table 3). This test determined the probability that the samples of L_{dom} from the chaotic terrain (n = 15) and from the inter-mesa terrain (n – 23) derive from the same statistical population, based on the distribution of sample medians (Fig. 12). Probabilities associated with the non-parametric Mood's Median Test, which is less affected by outliers in the data than the U-Test, are quoted in brackets (Table 3). The null hypothesis, H_0 ($\alpha = 0.05$), was again that there is no significant difference in the medians of L_{dom} derived from the power spectra of the chaotic and inter-mesa terrain elevations. Failure to reject H_0 (no significant difference between the chaotic terrain and inter-mesa terrain median L_{dom}) would mean that, despite the morphological difference between the chaotic and inter-mesa terrains, their relief oscillates over the same horizontal interval, producing a spatial similarity in their patterns of relief.

2.2.4 *Tests to understand what determines L_{dom}.*

To confirm that chaotic terrain L_{dom} is a reliable measure of the horizontal scale over which trough-plateau-trough alternations in elevation occur, the maximum widths of 105 plateaus (w_p) in Galaxias Chaos were measured from the CTX imagery, along planes parallel to the elevation profiles. Then the medians of L_{dom} (chaotic terrain) and w_p,(Fig. 12) were compared

using the non-parametric Mann-Whitney U-Test and Mood's Median Test (Table 3). H_0 (α = 0.05) was that there is no significant difference in the medians of L_{dom} (chaotic terrain) and w_p. To consider L_{dom} (chaotic terrain) to have been imparted onto the Galaxias Chaos landscape by w_p, H_0 must not be rejected. If H_0 is rejected, the conclusion must be that L_{dom} (chaotic terrain) is not a proxy for w_p. If testing failed to reject H_0, the test was replicated on the data from Galaxias Mensae to test if L_{dom} (inter-mesa terrain) could have been imparted by landforms with similar horizontal dimensions to the plateaus (w_p) in the chaotic terrain. In this test, failure to reject H_0 (no significant difference between the medians of L_{dom} (inter-mesa terrain) and w_p, α = 0.05) would mean that the scale over which the cyclicity of inter-mesa relief operates and the physical size of chaotic terrain plateaus are the same (Table 3). This result would be consistent with the terrain of Galaxias Mensae being subdivided into relief units with the same fracture-orthogonal width as the plateaus in Galaxias Chaos.

This testing was replicated on the maximum widths of 68 mesas (w_m) in Galaxias Mensae; w_m was defined as maximum mesa width from escarpment base to escarpment base along a plane parallel to the elevation profiles. H_0 (α = 0.05) was that there is no significant difference in the medians of L_{dom} (inter-mesa terrain) and w_m. In this case, failure to reject H_0 would mean that the scale over which the cyclicity of inter-mesa relief operates and the physical size of mesas in Galaxias Chaos are the same (Table 3). This result would be consistent with the terrain of Galaxias Mensae being subdivided into relief units with the same fracture-orthogonal width as the mesas in the region. Clearly, failure to reject both H_0 (L_{dom} inter-mesa terrain *v* w_p) and H_0 (L_{dom} inter-mesa terrain *v* w_m), and finding no significant difference in the medians of w_p and

w_m, would be consistent with: (1) the relief cyclicity of the inter-mesa terrain having a statistically significant imprint of the former presence of chaotic terrain, and; (2) the extant mesas of Galaxias Mensae being relatively well-preserved chaotic terrain plateaus separated by expanses of degraded plateaus in the inter-mesas. The results of all the statistical tests, applied to the directional data (*1H*, *Section 2.2*) and the elevation profiles (*2H*), can provide an answer to research question 1 (*Section 1*); what was the total extent of landscape degradation involved in producing the present landscapes of Galaxias Chaos and Galaxias Mensae-Colles? Answering research question 2, concerning the possibility of liquid water having been a product of regional landscape degradation, required an interpretation of the quantitative analyses within an overarching landscape context based on qualitative observations.

3 OBSERVATIONS

3.1 Overview from preliminary observations

While acknowledging the geomorphological differences between Galaxias Chaos and Galaxias Mensae-Colles (Pedersen and Head, 2010), this paper was stimulated by the following observations, which suggested that deeper insights could be gained regarding the spatiality and mechanisms of devolatization involved in landscape evolution within and between the Galaxias regions. (1) The edges of plateaus in Galaxias Chaos (Fig. 2A) appear to have a similar directional arrangement to the edges of mesas in Galaxias Mensae and Galaxias Colles (Fig. 2B, 2C). (2) Assemblages of mesas in Galaxias Mensae (Fig. 3A) appear to be directionally organised. (3) The mesas of Galaxias Mensae occur within the same elevation range as the neighbouring chaotic terrain of Galaxias Chaos (Fig. 3B). (4) The thickness of mesas in Galaxias Mensae is of the same

order as the thickness of chaotic terrain plateaus in neighbouring Galaxias Chaos (Fig. 3B). (5) Although the inter-mesa terrain of Galaxias Mensae appears largely devoid of distinct landforms in visible-wavelength images, HRSC elevation profiles of the inter-mesas suggest subtle, repeating oscillations (i.e. cyclicity) in elevation; these apparent oscillations look like vertically truncated, subdued versions of the trough-plateau-trough alternations in the chaotic terrain of Galaxias Chaos (Fig. 3B). (6) The inter-mesas of Galaxias Mensae appear to have a topography of alternating steeper and gentler slope units (Fig. 3C) that, together with the apparent cyclicity in elevation, suggest that subtle, degraded mesas could exist in the terrain between extant mesas. (7) While most of Galaxias Chaos is characterised by angular plateaus bounded by trough-fractures (Fig. 4A), its northern margin is characterised by increasingly degraded plateaus, resembling the mesas of Galaxias Mensae (Fig. 2A, 2B, 3A). (8) In addition to short inter-plateau fractures, long parallel fractures pervade Galaxias Chaos (Fig. 4A, arrowed) with both the same SE-NW strike and spacing as the fractures that cross Galaxias Fossae and Galaxias Mensae (Fig. 1A and B). At the head of Galaxias Fossae, between Galaxias Chaos and Galaxias Mensae, the fractures pervading a mesa assemblage, which closely resembles chaotic terrain, impart a cross-cutting radial-concentric pattern (Fig. 4B, examples labelled). Although apparently deviating from the usual SE-NW orientation, the convergence of the radials to the NW, towards a rubbly area of heavily degraded mesas, maintains the pattern; the SE-NW fractures of Galaxias Fossae originate from this convergence area (Fig. 4B). Likewise, to the north of the mesa assemblage, long chains of pitted cones trend towards the head of Galaxias Fossae (Fig. 4B, examples arrowed). The inter-mesas of Galaxias Mensae are regularly partitioned into parallel swaths by the SE-NW fractures (Fig. 4C - F). (9) Short fractures striking SW-NE pervade mesas in Galaxias

Mensae (Fig, 4C, mesas marked V and W); together, the main SE-NW fractures and the shorter SW-NE fractures dissect the landscape, with an arrangement mirrored by the geometry of the free-standing mesas; in Fig 4C, arrowed mesa edges are located alongside SE-NW fractures, some of which strike between closely-spaced mesas (Fig. 4B - D). (10) In Galaxias Mensae, many inter-mesas are partitioned by bilateral intersections and into quadrilateral blocks by chains of pitted cones with the same SE-NW/SW-NE orthogonal arrangement (Fig. 4D, pitted cone chains are arrowed). (11) Where inter-mesa pitted cone chains terminate abruptly at mesas, fractures propagate through the mesas directly along-strike from the cone chain termini (Fig. 4D, fracture arrowed at X). (12) The escarpments of many mesas are directly aligned with fractures striking alongside (Fig. 4C, 4E, mesa arrowed) but the tilt of some mesas and the angular difference between the strikes of the mesa and inter-mesa fractures suggest that the mesa-forming unit was susceptible to settlement disturbance and partial rotation (Fig. 4E, marked Y); near this example, a pit within a small crater (enlarged in box Y, Fig 4E) indicates there are voids in the subsurface, which, if present extensively, could contribute to instability in the overlying, mesa-forming, unit. Less than 5 km south of the pitted-crater, three small mesas are arranged around, and tilt away from, a set of fractures mutually separated by ~120° of arc (Fig, 4E, short arrow). This arrangement suggests that the fractures opened as a consequence of tension due to settlement around the periphery of the mesa group, another example of surface form developing from subsurface disturbance. (13) The fractured unit is, in places, almost completely devoid of overlying mesas but, even in these areas, highly degraded, but fracture-aligned, mesas remain apparent (Fig. 4 F, arrowed Z). In addition, rounded hummocks are pervaded by fractures or by short chains of pitted cones oriented either parallel or orthogonal to the

fractures (Fig. 4F, fractured hummock and cone-pervaded hummocks arrowed). (14) Similarly, in Galaxias Colles, there appears to be a close relationship between the disposition of knobs and the dominantly ESE-WNW strike of the dark lineaments (Fig. 5).

Together, these observations suggest that, while the landscapes of the Galaxias regions are morphologically distinct, their characteristic chaotic, mesa, or knobby terrains appear to share directional arrangements corresponding to the same partitioning in the substrate; in places, this involves ground disturbance and fracturing associated with settlement. These directional arrangements are maintained in mesas of varying states of degradation. The detailed observations, measurements and analyses that follow were performed to provide a more rigorous description of the regional landscapes, allowing these preliminary observations to be evaluated and the hypotheses tested. If substantiated, the implications would be that: an extremely large volume of surficial materials, probably containing a significant amount of water stored as ice, has been removed from Galaxias Mensae, possibly Galaxias Colles too, in the process of morphological divergence from Galaxias Chaos, and; that inherited characteristics of, or active processes within, the sub-mesa fractured unit played a role in the partitioning and degradation of Galaxias Mensae and Galaxias Colles.

3.2 Chaotic, mesa and knobby terrains

Galaxias Chaos (Fig. 2A, 3) is characterised by planar surfaces cross-cut by intersecting fractures, producing closely-spaced, low-relief, free-standing plateaus. Layering is apparent along exposed plateau edges (Fig. 4). The plateaus range in width from ~1 – 14 km, with separations of ~0.3 – 3 km, and fracture floor to surface relief between ~100 and 250 m (e.g. Fig. 3B).

Mesas occur throughout Galaxias Mensae and range in width from ~1 – 9 km. Unlike the closely-spaced plateaus of Galaxias Chaos, mesas generally have separations ranging from ~5 – 50 km. Like the chaotic terrain plateaus, the mesas are horizontally layered (Fig. 4). Some mesas form closely-spaced assemblages (Fig. 3A-D, 4B) separated internally by narrow fractures but between assemblages by wider corridors. In Galaxias Mensae, both the mesa assemblages the intervening inter-assemblage corridors have an orthogonal directionality, dominated by SE-NW and SW-NE arrangements (Fig. 3E). Galaxias Colles is characterised by mesas and knobby terrain - circular, elliptical and pyramidal hills, smaller than the mesas. Individual knobs rarely exceed 1.5 km across and occur in isolation, with spacings of ~2 – 20 km, or in assemblages with inter-knob spacings ranging from ~0.1 to <0.5 km (Fig. 2C).

The mesas of Galaxias Mensae and the chaotic terrain of Galaxias Chaos face each other across an intervening valley-form (the term not to implying a specific genesis, only a morphological characteristic) that contains the Galaxias Fossae assemblage of SE - NW striking fractures (Fig. 1, 3A, B). Across Galaxias Chaos to the furthest mesas of Galaxias Mensae (350 km), the elevations of chaotic plateaus and isolated mesas are closely accordant (Fig. 3B). The opposing populations

of chaotic plateaus and isolated mesas descend towards the axis of the Galaxias Fossae valley-form, having very similar vertical dimensions; less than 200 m, rarely 250 m, from chaotic block tops to fracture bottoms in Galaxias Chaos (Fig. 2A, 3B) and between mesa tops and the inter-mesa plain in Galaxias Mensae and Galaxias Colles, (Fig. 3B).

3.3 Fractures and dark lineaments

Fractures ~10 km to >200 km long strike SE - NW through Galaxias Chaos, Galaxias Mensae and Galaxias Fossae (Fig. 4). The SE-NW strike of the fractures (Fig. 9) is orthogonal to the regional-scale contours (Fig. 1B). In Galaxias Mensae, the terrain between the SE-NW fractures is in places subdivided by smaller, cross-cutting, secondary fractures (Fig. 4). Fractures in Galaxias Mensae and Galaxias Fossae are overlain by intact mesas but pervade some mesas (Fig. 4A, C-F). Other fractures, including cross-cutting secondary fractures, strike directly along the edges of mesas. Some fractures in Galaxias Mensae (Fig. 4) and Galaxias Fossae (Fig. 6) either bound or pass under mesas and are occupied by chains of pitted cones (*Section 3.5*).

The plains of northern Galaxias Colles, below an elevation of -3500 m, are patterned by dark lineaments up to ~360 km long and striking (E)SE-(W)NW (Fig. 9), orthogonal to the regional-scale contours. The dark lineaments cross plains sparsely relieved by mesas and knobs, which are often arranged like nodes along the lineaments or in tracts parallel to adjacent lineaments (Fig. 5). The dark lineaments are bounded to the south by a more densely populated mesa-knob landscape, the elevation of which varies only by the thickness of individual mesas and knobs (Fig. 1, 5).

3.4 Fractures evolving to the Galaxias Fossae distal channel

In Galaxias Fossae/Galaxias Mensae, at elevations between -3900 m and -4000 m, segments of 5 neighbouring primary fractures (Fig. 6, Fractures A-E) are linked by curving secondary fractures. Fracture F (Fig. 6), to their SW at a lower elevation, has no curving secondary. Together, Fractures A-E partition several closely-spaced mesas. Each fracture contains a chain of large (700 m wide) pitted cones, some of which can be seen emerging from beneath adjacent mesas (Fig. 6). Secondary fractures strike along local slopes, from a maximum elevation at the junction with their primary, to either an unlinked terminus or to join another cross-cutting primary (e.g. between Fracture A and B) at a lower elevation. The primary fractures descend gradually to the NW. Fracture A ultimately attains the lowest elevation and, in doing so, captures Fractures B and E (Fig. 6). At elevations greater than its point of capture, fracture E occupies the hypsometric axis of the valley-form. At elevations lower than this capture (-4100 m), Fracture A becomes the hypsometric axis of the Galaxias Fossae valley-form (Fig. 1, 6). The terrain between Fractures A-E, and bounding the distal reaches of Fracture A (a distance >200 km), is compartmented into 5 - 6 km-wide blocks by cross-cutting chains of pits, fractures, trenches and troughs (Fig. 6). Together, these forms produce a system of trellis-pattern chasms that open into Fracture A as channels (Fig. 6).

The transition from straight primary fractures to curving fractures containing pitted cones, and also to Fracture A becoming the dominant regional fracture of Galaxias Fossae, starts at -4000 m elevation and is complete by -4200 m. This also is the elevation at which Fracture A transitions to having a deepened-widened, channel-like morphology (Fig. 6). From this transition, the

Fracture A channel is extremely straight and flat (Fig. 1B), extending for ~220 km onto the surrounding plain before developing a sinuous planform. Also at -4000 m, from SE-NW elongated pits and fractures on the flanks of Elysium Mons, Hrad Vallis emerges as a meandering channel (Fig. 1). The terrain between Hrad Vallis and Fracture A is regularly partitioned by parallel SE-NW striking fractures. The elongated Hrad Vallis source pits are linked with fractures up to 50 km long, striking parallel to the long SE-NW fractures running through Galaxias Chaos, 70 – 125 km to the east. The elevation of the highest Hrad Vallis source fractures, -3600 m, is accordant with the backwalls of Galaxias Chaos, 285 km distant. Hence, across this extensive region, a transition from parallel fractures and elongated pits to open channels occurs at ~-4000 m, with fractures, chaotic terrain and mesas up to -3600 m.

3.5 Fracture-bound pitted cones and pits.

Chains of pitted cones and pits within fractures emerge from beneath mesas surrounding the higher reaches of Fracture A. Where chains of pitted cones converge on Fracture A, approaching the hypsometric axis of the Galaxias Fossae valley-form, the fracture-cone systems develop curving transitions from primary (SE-NW) to secondary (SW-NE) alignment (Fig. 6). Within the fractures, it is apparent that the pitted cones and pits are differentiated only by their degree of exposure: fracture traces are pitted; deep fractures between mesas reveal cones and lower-lying pits (Fig. 6). Where overlying mesas have been nearly fully removed, variably-mantled pitted cones are revealed in fractures pervading the inter-mesa surface; where chaos-like mesas have been only thinned, not completely removed, pits are visible but not cones (Fig. 6). Consequently, the inter-mesa surface is geometrically partitioned by fracture-bound pitted

cone and pit chains into blocks with similar dimensions and planform as nearby mesas (Fig. 4B-E, 6). The resulting partitioning of the inter-mesa surface into blocks bounded by intersecting depressions is also very similar to the geometric partitioning characterising Galaxias Chaos.

3.6 Chains of pitted cones, broad ridges with cones.

The Galaxias Mensae inter-mesa surface is relieved by clusters and chains (3 – 4 km long, maximum) of pitted cones, individually up to 300 m in diameter (Fig. 7). Chains and clusters of pitted cones also occur along the apex of broad curving ridges, up to 5 km wide. Some ridges are fractured along their summits, revealing partially exposed pitted cones (Fig. 7). Cones up to 0.5 km diameter occur also in shorter chains (2 - 5 individuals) and tight clusters. The pitted cone chains stratigraphically underlie the mesa-forming unit and define the perimeter of some mesas (Fig. 6). In places, pitted cone chains superpose underlying primary fractures, having been fractured along the fracture trace (Fig. 7).

3.7 Softened terrain.

Between Galaxias Mensae and Galaxias Colles, some SE-NW primary fractures and chaotic-like mesas are apparent. However, these mesas are separated by intervening lobes of texturally "softened" caps, edged by curving ridges, chains of pitted cones or mounds (Fig. 8). Some convergences involved the over-riding of one lobe by another (Fig. 8). The softened appearance of the cap results from a lack of pervading fractures and planar, angular to sub-angular, mesas. However, some pitted cones that emerge through caps are marginally overlain by trailing lobes (Fig. 8).

4. Testing for landform directional correspondence within and between Galaxias Chaos and Galaxias Mensae

4.1 *Chaos block edges, mesa edges, mesa assemblage/inter-assemblage corridors*

The directional distributions of plateau edges (Fig. 9) in Galaxias Chaos and mesa edges in Galaxias Mensae and Galaxias Colles are non-uniform (*p(uniform)* ≤ 0 0008). The dominant edge orientations are bimodal: Galaxias Chaos, SE-NW/SSW-NNE; Galaxias Mensae, SE-NW/SW-NE; Galaxias Colles, ESE-WNW/SSW-NNE (Fig. 9). Like the edges of individual mesas, the mesa assemblages and inter-assemblage corridors in Galaxias Mensae (Fig. 3D, E) also have a statistically significant bimodal SE-NW/SW-NE directional distribution, *p(uniform)* ≤ 1.5×10^{-11}).

The Mardia-Watson-Wheeler W-Test for equal distributions failed to reject H_0 (no significant difference in directional distribution, $\alpha = 0.05$) in all pairwise tests (Table 2).Hence, the plateau edges in Galaxias Chaos, mesa edges in Galaxias Mensae-Colles, and both mesa assemblages and inter-assemblage corridors in Galaxias Mensae cannot be statistically differentiated on the basis of their directional arrangement. Moreover, this arrangement is weighted to azimuths parallel or orthogonal to the strike direction of the fractures and dark lineaments.

	Plateau Edges G. Chaos	Mesa Edges G. Mensae	Mesa Edges G. Colles	Mesa Assemblages G. Mensae
Mesa Edges G. Mensae	0.35			
Mesa Edges G. Colles	0.81	0.2		
Mesa Assemblages (G. Mensae)	0.11	0.88	0.39	
Inter-mesa Corridors (G. Mensae)	0.86	0.31	0.75	0.17

Table 2. Probabilities (*p*) of listed feature having the same directional distribution; pairwise testing of H_0 with the Mardia-Watson-Wheeler B-Test for equal distributions. To reject H_0, *p* must not exceed 0.05. Hence, H_0 is not rejected for any pairwise combination of features.

4.2 *Chains of pitted cones and broad ridges with cones.*

The orientation of pitted cone chains in Galaxias Mensae is non-uniform (Rao's U, *p*(*uniform*) = 0.008). The largest proportion of pitted cone chains (25%) is oriented SW-NE (45° – 225°), with the anti-mode of their directional distribution in the SE-NW sector (Fig. 9). The orientation of broad ridges also is non-uniform; *p*(*uniform*) = 0.03, the largest proportion (25 %) occupying the 345° - 165° sector (Fig.9). In the locations where broad ridges developed near the head of the Galaxias Fossae valley-form, this orientation is orthogonal to the local contours (Fig. 1B, 7).

4.3 Overview of the directional arrangements

The fracture strikes of Galaxias Chaos and Galaxias Mensae-Fossae are distinctly mutually parallel (Fig. 9), all dominantly SE-NW; in Galaxias Mensae, this strike direction is orthogonal to

regional-scale contours, which describe a landscape sloping gently to the NW but modified by relative steepening towards the Galaxias Fossae valley-form, focused on Fracture A (Fig. 1B, and 3B). The pitted cone chains are distinctly orthogonal to the primary fractures and regional slope in Galaxias Mensae-Fossae (and Galaxias Chaos). Rather, the pitted cone chains descend towards the Galaxias Fossae valley-form centered on Fracture A. In the restricted area in which broad ridges occur, they too are oriented down the local slope towards the head of the valley-form. Together, therefore, the primary fractures and pitted cone chains impart an orthogonal fabric (SE-NW/SW-NE) to the landscape of Galaxias Mensae, which is mirrored by the same orthogonal directionality in the mesa edges, mesa assemblages and inter-assemblage corridors in the region. All told, the geomorphologies of the chaotic terrain and mesa terrain units are underpinned by a simple directional organization, dominated by the fracture strike, the steepening of slopes towards the Galaxias Fossae valley form and, in Galaxias Mensae, the cross-cutting relationship between the fractures and the pitted cone chains.

5 Testing for the presence of degraded remnant mesas in Galaxias Mensae

5.1 Cyclical oscillation of elevation and mesa width in Galaxias Chaos

All power spectra derived from the 15 detrended elevation profiles (d = 1) from Galaxias Chaos are non-random ($p > 0.05$; Fig. 10A), with median L_{dom} = 3298 m (Fig. 12). Median w_p (105 measures) = 3235 m (Fig. 12). The Mann-Whitney U-Test failed to reject H_0 , stating no significant difference between median L_{dom} and median w_p; $p(same\ median) = 0.24$ (Mood's median test, $p = 0.84$). Formally, this result means that L_{dom} and w_p have the same spatial scale but is consistent with the interpretation that L_{dom} has been imparted by w_p.

	G. Chaos L_{dom}	G. Chaos w_p	G. Mensae L_{dom}
G. Chaos w_p	0.84 (0.78)		
G. Mensae L_{dom}	0.22 (0.38)	0.06 (0.15)	
G. Mensae w_m	0.48 (0.42)	0.06 (0.11)	0.47 (0.62

Table 3. Probabilities (*p*) of listed parameters having the same median; pairwise testing of H_0 with the Mann-Whitney U-Test for equal medians and, in brackets, Mood's median test. To reject H_0, *p* must not exceed 0.05. Hence, H_0 is not rejected for any pairwise combination of parameters.

5.2 Cyclical oscillation of inter-mesa elevation and mesa width within Galaxias Mensae and between Galaxias Mensae and Galaxias Chaos.

All power spectra derived from 23 detrended (d = 1) inter-mesa elevation profiles from Galaxias Mensae are non-random (p >0.05; Fig. 10B), median L_{dom} = 4421 m (Fig. 12). Median w_m (68 measures) = 3632 m (Fig. 12). The Mann-Whitney U-Test failed to reject H_0 (no significant difference between median L_{dom} and median w_m); *p*(*same median*) = 0.47 (Mood's median test, p = 0.62). Likewise, the measures of L_{dom} from both Galaxias Mensae inter-mesas and Galaxias Chaos show no significant difference in median; *p*(*same median*) = 0.22 (Mood's median test, p = 0.38). Neither are the medians of w_m (Galaxias Mensae mesas) and w_p (Galaxias Chaos plateaus) significantly different; *p*(*same median*) = 0.06 (Mood's median test, p = 0.11).

Given that the tests failed to reject all pairwise H_0, the hypotheses that relief of the inter-mesas of Galaxias Mensae oscillates with the same cyclicity as the chaotic terrain in Galaxias Chaos, and that this cyclicity corresponds with the width of the chaotic plateaus in Galaxias Chaos (w_p) and extant mesas (w_m) in Galaxias Mensae, have not been falsified. Given that w_p and w_m are not significantly different, this result indicates that, despite apparent morphological differences, the structuring of relief in Galaxias Chaos and Galaxias Mensae is monotonic, both regions sharing similarly scaled cyclic relief patterns.

5.3 Conclusions from the statistical analyses.

The analyses of landform directionality and relief cyclicity are the basis of an answer to research question 1 *via* a falsification of fundamental hypotheses *1H*; the extent of each Galaxias region cannot be determined on the basis of identifying the spatial distributions of distinct regional landform assemblages, differentiated on the basis of quantifiably distinct directional arrangements. The falsification of *2H* provides further insights; the relief of Galaxias Chaos is not quantifiably distinct, despite the morphological difference between its chaotic terrain and the mesa terrain of Galaxias Mensae. The directionality of chaotic terrain plateau edges and mesa edges (in both Galaxias Mensae and Galaxias Colles; *Section 4.3*) are not significantly different from each other. Also, there is a consistent pairwise correspondence between w_p, w_m, L_{dom} (chaotic terrain) and L_{dom} (inter-mesa terrain) (*Section 5*).On the basis of these results, the inference made is that the present landscape of Galaxias Mensae is a consequence of widespread degradation of a former cover unit that was partitioned identically, both directionally and with respect to relief oscillation, to the chaotic terrain of Galaxias Chaos.

Arising from this inference, a valid working hypothesis is that chaotic terrain most likely formerly extended from Galaxias Chaos across Galaxias Mensae, and possibly across Galaxias Colles, but has now been heavily degraded.

6. GEOMORPHOLOGICAL INFERENCES AND INTERPRETATIONS

6.1 Continuity of the Chaos/Mensae/Colles system

We infer that Galaxias Chaos/Mensae/Colles forms a coherent landsystem, based on the following findings. (1) There is a close correspondence between the thickness (~200 m) and internal, layered, structure of the mesa-forming unit of Galaxias Mensae and the chaotic terrain of Galaxias Chaos (*Section 3.1 and 3.2*). (2) The strikes of primary fractures in Galaxias Chaos, Galaxias Mensae and Galaxias Fossae are statistically concentrated along the same SE-NW plane (*Section 3.3*). The dark lineaments in Galaxias Colles are concentrated along an ESE-WNW plane (*Section 3.3*). (3) The primary fractures and dark lineaments strike along gentle regional slopes over distances of 10^2 km. (4) The orientations of chaotic terrain plateau edges in Galaxias Chaos and mesa edges in Galaxias Mensae and Galaxias Colles comprise a single statistical population (*Section 4.1 and 4.3*) dominated by alignments either parallel or normal to the strike of the primary fractures. (5) Pitted cone chains developed dominantly normal to the primary fractures (*Section 4.2 and 4.3*), downslope towards Fracture A, although some developed within primary fractures. (6) The dominant cyclicity (L_{dom}) of chaotic terrain relief in Galaxias Chaos corresponds with the maximum width of chaotic terrain plateaus (w_p) (*Section 5.1*).The dominant cyclicity (L_{dom}) of inter-mesa relief corresponds with both the dominant relief cyclicity of the chaotic terrain and the maximum width (w_m) of mesas in Galaxias Mensae (*Section 5.2*). This set of

mutual correspondences is consistent with the hypothesis that the mesas are a remnant of chaotic terrain that once extended across Galaxias Mensae; the relief cyclicity of the inter-mesas retains this imprint (*Section 5.3*). The pairwise correspondence in L_{dom}, w_p and w_m between Galaxias Chaos and Galaxias Mensae, together with the chaotic terrain plateaus and mesas in those regions having the same directional distribution, indicates that the former chaotic terrain plateaus of Galaxias Mensae had the same dimensions and spatial arrangement as the extant plateaus in Galaxias Chaos. From the GIS, based on MOLA MEGDR elevation data and landform mapping, cut and fill analysis of the extant chaotic terrain and mesa-knob-plains landscapes (Fig. 1) shows they have a combined surface area of ~440000 km^2, of which ~286400 km^2 have experienced net denudation (including by fracturing in the chaotic terrain). In total, the denuded area has lost a volume of ~22100 km^3, indicative of the removal of a unit with a mean thickness of 77 m. This tallies well with typical mesa thickness being less than 200 m, only rarely 250 m (Fig. 3B and *Sections 3.1, 3.2*). It is impossible to determine accurately the ice-to-lithic ratio of the remnant inter-mesa lag deposit, but the likelihood is that the proportion of lithics in the lag has increased passively, owing to the preferential removal of ice. Even allowing for an unchanged ice-to-lithic ratio in the lag deposit, and assuming an original ice content of 50 – 85 vol%, the same as estimated for western Utopia Planitia by Stuurman et al. (2016), ≥ 11000 km^3 of ice could have been removed as a consequence of the surface degradation in the Galaxias regions; by comparison, the Vatnajokull ice cap in Iceland has a volume of ~3200 km^3.

6.2. Assessing the possible role of water in regional landscape evolution - research question 2.

Based on the directional arrangement of the landforms described and analysed (*Sections 3, 4*), and the spatial cyclicity of their relief, this section aims to deduce the key processes involved in the evolution of the inter-regional landscapes of Galaxias. A key focus will be an attempt to construct a genetic hypothesis that is consistent with the differences between the present landscapes but: (1) the relief-forming components of Galaxias Chaos, Galaxias Mensae and Galaxias Colles having the same directional characteristics, and;(2) the relief of Galaxias Chaos and Galaxias Mensae having the same cyclicity.

6.2.1 *The Galaxias Fossae valley-form and Galaxias Mensae*.

The SE-NW primary fractures in Galaxias Mensae strike parallel to the axis of the Galaxias Fossae valley-form. The continuation of the primary fractures onto the plains beyond any morphological expression of the valley-form (Fig. 1), suggests that the fractures are independent of the valley-form. Rather, the valley-form developed along the strike of regionally extensive fractures, post-dating their emplacement. The pitted cones in Fracture A developed where the fracture became the focus of adjacent primary fractures (B-E and F), *via* curving secondary fractures and fracture-cone chains, troughs, trenches, coalesced pits and, ultimately, channel-like chasms (Fig. 6).

The pitted cones in secondary fractures joining fracture-channel A (Fig. 6) evolve towards the fracture from pitted cones, to pits and, finally, channels that developed by the coalescence of pits. This morphological and network evolution is consistent with the gravity-directed

transmission of a liquid, ending in a transition from subsurface to subaerial discharges into fracture-channel A (Fig. 6). The distribution, orientation and extent of pitted cones suggests that they represent widespread underground conduits, each cone being the locus of an upward movement of pressurized liquid carrying and depositing sediment or becoming a solid as it reached the surface. If the pitted cones represent the intermittent puncturing of underground conduits by upward injections of pressurized liquid, they have an analogous nodal-linear morphology to volcanic fissure vents or chains of landforms related to hydrovolcanic or cryovolcanic phreatomagmatic eruptions, including rootless cones (Bruno et al., 2004, 2006) and mud volcanoes (Skinner and Tanaka, 2007). The cones in Galaxias do not appear to be cinder cones (Plescia, 1980), as vent or flank lava flows are absent (*cf.* Lanz and Saric, 2009). The significance of rootless cones and mud volcanoes is that they indicate past interactions between lava and either ground-ice or groundwater (Hamilton et al., 2010, 2011).

In Galaxias Mensae, broad curving ridges are of the same scale as pitted cones chains. Pitted cones and longitudinal fractures occur along the summit of some broad ridges or adjacent to them (Fig. 7). Some pitted cone chains develop along ridge-summit longitudinal fractures (Fig. 7). The summital fractures suggest that the broad curving ridges experienced uplift, dilation and axis-normal (lateral) tension. The development of associated pitted cones is consistent with the occurrence of nodal pressurization at points along the ridges. In contrast to pitted cone chains, the broad ridges probably developed at greater depth and, consequently, had thicker cover, sufficiently competent generally to resist eruption or effusion. The presence of swellings along the broad ridges (e.g. Fig. 7) suggests that they experienced longitudinally intermittent dilation

without fracturing. By contrast, shallower underground conduits became open to the atmosphere by rupture or collapse (Fig. 4, 6).

The only location where a transition from primary fractures to open channels occurred was in the trellised subaerial chasm network in the convergence zone of Fractures B-E with Fracture A (Fig. 6). A similar, though topologically simpler, subsurface to subaerial transition occurred along the upper reaches of Hrad Vallis, which developed into a channel from linear fractures and pits. The Galaxias Fossae-Mensae landscape could represent the former operation of two discharge regimes: (i) an upland, subsurface, high fluid-pressure regime at elevations of between ca. -3600 m and -4000 m, where pitted cone chains and broad curving ridges formed, and; (ii) a subaerial regime below -4000 m. Overall, because of the focusing of discharge through Fracture A, it became the regional focus of landscape lowering and, consequently, the axis of the Galaxias Fossae valley-form.

6.2.2 *Galaxias Colles.*

With respect to the dark lineaments in Galaxias Colles, their hypsometric, directional (i.e. near-parallel to the strike of primary fractures and orthogonal to regional contours) and stratigraphic (i.e. overlain by the mesa-unit) characteristics suggest that they are primary fractures. The presence of extensive sets of primary fractures, separated by hundreds of kilometers but having very similar geometries, suggests that the primary fractures and dark lineaments could be consequences of uplift and tensional adjustment across all the Galaxias regions (Chaos, Mensae, Colles). If so, the fractures probably the surface expression of dikes reflecting fundamental

processes of high-order relief production associated with either the updoming of Tharsis or Elysium Mons volcanism, possibly both (Carr, 1974; Hall et al., 1986; Wilson and Head, 2002).

6.2.3 Terrestrial and Martian analogues of pitted cones as surface expressions of upwelling fluid.

The form, stratigraphic characteristics and apparent competence of the pitted cones are consistent with them being the tops of dikes (Pedersen et al. 2010) or pipes through which fluidized material was injected from depth. In volcanic regions on Earth, when magmas intrude deposits containing ice or water, rapid phase changes cause ground fracturing and the eruption of steam from vents along the fracture zone; rootless cones commonly form as result of the eruptions, often followed by mud volcanism as the system cools (Lanz and Saric, 2009).

On Mars, pitted cones have been interpreted as rootless cones (Lanagan et al., 2001; Fagents et al., 2002] and mud volcanoes (Skinner and Tanaka, 2007; Oehler and Allen, 2010; Komatsu et al., 2012), in either case implying hydrovolcanism or cryo-volcanism (*cf*. Hamilton et al., 2010, 2011). However, stratabound injection of liquefied clastic material through vertical pipes can occur without the production of mud volcanoes, in association with hydrothermal and seismic processes; in this instance, assemblages of pitted cones may form due to erosion of capping layers and the more rapid weathering and erosion of exposed pipe interiors in contrast to cemented pipe walls (Netoff and Shroba, 2001. The absence of clear outflow channels or lobate flows from the pitted cones in Galaxias Mensae suggests that, if they were associated with thermal fluid generation, the injectite was largely accommodated within or below the overlying mesa-forming surface unit, perhaps by pore-space filling, without significant organised outflow.

This suggests that the pitted cones most likely represent the tops of injection pipes exposed by subsequent erosion of overburden.

6.3 Regional synthesis.

Both the morphology and directional arrangement of the characteristic regional landform assemblages, and the finding of no statistically significant difference between the cyclicity of relief in Galaxias Chaos and Galaxias Mensae, support the interpretation of regional divergence in the evolution of morphology but not separate regional origins. Galaxias Mensae has retained remnant chaotic terrain in the form of its mesas, mesa assemblages and spatial cyclicity of inter-mesa relief. In losing much of its chaotic-terrain surface, a unit up to ~200 m thick, Galaxias Mensae has evolved towards a plains morphology but retains the same underlying cyclicity of relief as Galaxias Chaos. Therefore, in attempting to account for the greater degree of degradation in Galaxias Mensae and Galaxias Colles than in Galaxias Chaos, mechanisms need to be considered that are genetically consistent both with the regional landform assemblages and their spatial divergence.

Fracture A

The focusing of discharge to a very specific sink from distributed sources led to an intense eradication of terrain, including unroofing of conduits, between fracture-channel A and adjacent primary fractures.

Pitted cones

Pitted cones developed in a stratigraphic unit overlying the primary fractures; the cone-forming unit developed grabens, and individual cones collapsed, along the traces of the underlying primary fractures (Fig. 7). The directional fabric of the landscape reflects the geometry of the primary fractures and the development of crossing orthogonal conduits that intermittently produced cones. Chains of pitted cones reflect the injection of this liquid, under pressure, into the overlying, ultimately mesa-forming, unit.

The areal denudation of the Galaxias Mensae and Galaxias Colles was compartmented by the collapse or deflation of the surface along the traces of the resulting intersecting fracture-conduit planes. According to the lack of statistical difference in the cyclicity of relief in Galaxias Mensae and Galaxias Chaos, it is likely that the degraded surface of Galaxias Mensae was formerly partitioned into chaotic terrain dominated by plateaus ~3 km wide.

The morphology of the softened terrain caps in Galaxias Mensae is consistent with them having collapsed and spread as a consequence of radial sliding over a lubricated shear plane. Given the regional context, a likely source of this liquid was the degradation of a near-surface icy unit, destabilized by the provision of volcanically generated ground heat. Hence, we suggest that the pitted cones are best interpreted as injection pipes that transmitted hydrothermally fluidized material along and into the base of the overlying, ultimately mesa-forming unit. Where the mesa-forming unit was thinned sufficiently by basal thermal degradation, injection pipes emerged to form pitted cones (*cf.* Netoff and Shroba, 2001). We acknowledge that this morphogenetic interpretation stems from the occurrence of icy surface materials in a generally

volcanic landscape context, rather than the observation of landforms unequivocally diagnostic of the production of thermally-generated groundwater. Alternatively, some of the landforms could be explained as having resulted from the lateral transmission of low viscosity lavas (Hopper and Leverington, 2014), rather than groundwater. Hence, we present our preferred interpretation as a working hypothesis that has not yet been falsified - but both hypotheses need further testing. The findings of this paper suggest that future research should focus on the region with the greatest concentration of pitted cones, broad ridges and texturally softened terrain. These landforms probably map centres of ground heating and associated sources of fluid flow, either endogenically generated groundwater or low viscosity lava.

7. Conclusions

In answer to research question 1, the observations and analyses in this paper suggest that terrain with the same directional pattern and relief as presently found in Galaxias Chaos, probably chaotic terrain, formerly extended across Galaxias Mensae and Galaxias Colles. The total extent of this terrain was ~440000 km^2 but ~22000 km^3, averaging 77 m thick, have been lost across an area of ~285000 km^2. Assuming this material had the same icy composition as the mesa-forming unit in western Utopia Planitia characterized by Stuurman et al., (2016) ≥ 11000 km^3 of ice could have been removed as a consequence of the surface degradation. Galaxias Chaos became morphologically differentiated from Galaxias Mensae-Colles through spatially variable modes of surface degradation. If nothing else, these findings are indicative of a significant loss of ice-bearing deposits from Galaxias Mensae-Colles. However, this regional landscape is consistent with the surface degradation having occurred in locations characterised

by landforms associated with elevated ground heating and the transmission of a fluid in the shallow subsurface towards a distal discharge channel. It cannot be determined definitively if the fluid involved was groundwater, generated by the thermal destabilisation of icy near-surface materials, or low viscosity lava. Therefore, in answer to research question 2, the generation of significant quantities of cryo-volcanic groundwater cannot be ruled out as a consequence of regional landscape evolution but it is likely that the degradation of Galaxias Mensae-Colles was not a consequence of sublimation alone. This research paints a more complex picture of total landscape evolution than consideration of intact chaotic terrain alone and underscores the significance of cryo-volcanic interactions in the cycling of water between the Martian surface and the atmosphere.

ACKNOWLEDGEMENTS

The authors sincerely thank Pete Mouginis-Mark and an anonymous referee for the efforts they invested in reviewing this paper and the insights and improvements they offered, which significantly improved it. Thanks also to Jim Skinner for the time, insights and advice he generously contributed to this paper.

REFERENCES

Carr, M. H. (1974). Tectonism and volcanism of the Tharsis Region of Mars, *J. Geophys. Res*., 79(26), 3943–3949, doi:10.1029/JB079i026p03943.

Carr, M. and Schaber, G.G. (1977). Martian permafrost features. *J. Geophys. Res*., 82 (28), 4039–4054.

Carr, M. (1979). Formation of martian flood features by release of water from confined aquifers, *J. Geophys. Res.*, 84, 2995–3007.

Carr, M.H. (1996). *Water on Mars*, Oxford Univ. Press, New York. 229 p.

Carr, M. and Head, J.W. (2003). Oceans on Mars: An assessment of the observational evidence and possible fate, *J. Geophys. Res*., 108 (E5). doi:10.1029/ 2002JE001963.

Christensen, P. R., Jakosky, B.M, Kieffer, H.H, Malin, M.C., McSween, H.Y., Nealson, K., Mehall, G.L., Silverman, S.H., Ferry, S., Caplinger, M. and Ravine, M. (2004). The Thermal Emission Imaging System (THEMIS) for the Mars 2001 Odyssey Mission, *Space Sci. Rev*., 110, 85 – 130.

De Hon, R.A. (1992). Polygenetic origin of Hrad Vallis region of Mars. *Lunar Planet. Sci*. XXII, 45–51 (abstract).

De Pablo, M.A., Michael, G.G. and Centeno, J.D. (2013). Age and evolution of the lower NW flank of the Hecates Tholus volcano, Mars, based on crater size–frequency distribution on CTX images, *Icarus*, 226, 455-469. doi.org/10.1016/j.icarus.2013.05.012.

Gwinner, K., Scholten, F., Spiegel, M., Schmidt, R., Giese B., Oberst, J., Heipke, C., Jaumann, R. and Neukum, G. (2009). Derivation and Validation of High-Resolution Digital Terrain Models from Mars Express HRSC Data, *Photogrammetric Engineering and Remote Sensing*, 9, 1127-1142(16). doi:10.14358/PERS.75.9.1127.

Hamilton, C. W., S. A. Fagents, and L. Wilson (2010), Explosive lava-water interactions in Elysium Planitia, Mars: Geologic and thermodynamic constraints on the formation of the Tartarus Colles cone groups*, J. Geophys. Res*., 115, E09006. doi:10.1029/2009JE003546.

Hamilton, C. W., S. A. Fagents, and T. Thordarson (2011), Lava–ground ice interactions in Elysium Planitia, Mars: Geomorphological and geospatial analysis of the Tartarus Colles cone groups, J. Geophys. Res., 116, E03004. doi:10.1029/2010JE003657

Hammer, Ø., Harper, D.A.T. and Ryan, P.D. (2001). PAST: Paleontological Statistics Software Package for Education and Data Analysis, *Palaeontologia Electronica*, 4(1): 9pp.

Hammer, Ø. and Harper, D.A.T. (2006). *Paleontological Data Analysis*. Blackwell.

Hartmann, W. K. & Berman, D. C. Elysium Planitia lava flows' Crater count chronology and geological implications. *Journal of Geophysical Research* **105**(15), 011–15,025 (2000).

Hauber, E., van Gasselt, S., Ivanov, B., Werner, S., Head, J.W., Neukum, G.,Jaumann, R., Greeley, R., Mitchell, K., Muller, P., and the HRSC Co-Investigator Team (2005). Discovery of a flank caldera and very young glacial activity at Hecates Tholus, Mars, *Nature*, 434, 356–361. doi:10.1038/nature03423.

Jaumann, R., Neukum, G., Behnke, T., Duxbury, T.C., Eichentopf, K, Flohrer, J., v. Gasselt, S., Giese, B., Gwinner, K., Hauber, E., Hoffmann, H., Hoffmeister, A., Köhler, U., Matz, K.-D., McCord, T.B., Mertens, V., Oberst, J., Pischel, R., Reiss, D., Ress, E., Roatsch, T., Saiger, P., Scholten, F., Schwarz, G., Stephan, K., Wählisch, M., the HRSC Co-Investigator Team (2007). The high-resolution stereo camera (HRSC) experiment on Mars Express: Instrument aspects and experiment conduct from interplanetary cruise through the nominal mission, *Planetary and Space Science*, 55, 928–952.

Hopper, J. and Leverington, D. (2014). Formation of Hrad Vallis (Mars) by low viscosity lava flows. *Geomorphology*, 207. 96–113. 10.1016/j.geomorph.2013.10.029.

Komatsu, G., Okubo, C.H.,Wray, J.J, Gallagher, R., Orosei, R., Cardinale, M., Chan, M.A. and Ormö, J. (2012). Small mounds in Chryse Planitia, Mars: testing a mud volcano hypothesis, 43rd *Lunar and Planetary Science Conference*, Abstract 1103.

Lanagan, P. D., McEwen, A. S., Keszthelyi, L. P. and Thordarson, T. (2001). Rootless cones on Mars indicating the presence of shallow equatorial ground ice in recent times, *Geophys. Res. Lett.*,28, 2365–2368. doi:10.1029/2001GL012932.

Fagents, S. A., Lanagan, P. and Greeley, R. (2002). Rootless cones on Mars: A consequence of lava-ground ice interaction, in *Volcano-Ice Interaction on Earth and Mars*, edited by Smellie, J. L. and Chapman, M. G., *Geol. Soc. Spec. Publ*., 202, 295–317.

Lanz, J. K., and M. B. Saric (2009). Cone fields in SW Elysium Planitia: Hydrothermal venting on Mars? *J. Geophys. Res*., 114, E02008. doi:10.1029/2008JE003209.

Malin, M. C., et al. (2007). Context Camera Investigation on board the Mars Reconnaissance Orbiter, J. Geophys. Res., 112, E05S04, doi:10.1029/2006JE002808.

Mouginis-Mark, P.J. and Wilson, L. (2016). Possible Sub-Glacial Eruptions in the Galaxias Quadrangle, Mars, *Icarus*, 267, 68-85. doi.org/10.1016/j.icarus.2015.11.025

Netoff, D.I. and Shroba, R.R. (2001). Conical sandstone landforms cored with clastic pipes in Glen Canyon National Recreation Area, southeastern Utah, *Geomorphology*, 39, 99–110.

Oehler, D.Z. and Allen, C.C., (2010). Evidence for basin-wide mud volcanism in Acidalia Planitia, Mars.41st *Lunar and Planetary Science Conference*, Abstract 1009.

Pedersen, G.B.M. and Head, J.W. (2010). Evidence of widespread degraded Amazonian-aged ice-rich deposits in the transition between Elysium Rise and Utopia Planitia, Mars: Guidelines for the recognition of degraded ice-rich materials, *Planetary and Space Science*, 58, 1953–1970.

Pedersen, G.B.M., Head, J.W. and Wilson, L. (2010). Formation, erosion and exposure of Early Amazonian dikes, dike swarms and possible subglacial eruptions in the Elysium Rise/Utopia Basin Region, Mars, *Earth and Planetary Science Letters*, 294, 3–4, 424-439. doi.org/10.1016/j.epsl.2009.08.010.

Pedersen and Head, (2011). Chaos formation by sublimation of volatile-rich substrate: Evidence from Galaxias Chaos, Mars, *Icarus* 211, 316–329.

Platz, T. and Michael, G. (2011). Eruption history of the Elysium Volcanic Province, Mars. *Earth Planet. Sci. Lett*., 312, 140–151. http://dx.doi.org/10.1016/j.epsl.2011.10.001

Plescia, J. B. (1980). Reports of the Planetary Geology Program, 1980, *NASA Tech. Memo, NASA TM-82385*, 263–265.

Scott, D.H., and Carr, M.H., 1978, Geologic map of Mars: U.S. Geological Survey Miscellaneous Investigations Series Map I–1083, scale 1:25,000,000.

Sharp, R. (1973). Mars: Fretted and chaotic terrains, *J. Geophys. Res.*, 78, (20): 4073–4083, doi:10.1029/JB078i020p04073

Skinner, J. A., and K. L. Tanaka (2007), Evidence for and implications of sedimentary diapirism in the southern Utopia highland-lowland boundary plain, Mars, *Icarus*, 186, 41–59. doi:10.1016/j.icarus.2006.08.013

Smith, D. E. et al. (2001). Mars Orbiter Laser Altimeter: Experiment summary after the first year of global mapping of Mars, *Journal of Geophysical Research*, 106, 23689-23722. doi:10.1029/2000JE001364.

Stuurman, C. M., Osinski, G.R., Holt, J.W., Levy, J.S., Brothers, T.C., Kerrigan, M. and Campbell, B.A. (2016). SHARAD detection and characterization of subsurface water ice deposits in Utopia Planitia, Mars, *Geophys. Res. Lett.*, *43*, 9484–9491, doi:10.1002/2016GL070138.

Vaucher, J., Baratoux, D., Mangold, N., Pinet, P., Kurita, K. and Grégoire, M. (2009). The volcanic history of central Elysium Planitia: Implications for martian magmatism. *Icarus* **204**, 418–442.

Wilson, L. and Head, J. (2002). Tharsis-radial graben systems as the surface manifestation of plume-related dike intrusion complexes: models and implications. *Journal of Geophysical Research*, 107, 1-24. doi:10.1029/2001JE001593.

Wilson, L. and Mouginis-Mark, P.J. (2003). Phreatomagmatic explosive origin of Hrad Vallis, Mars, *J. Geophys. Res*., 108 (E8), 1–16. doi:10.1029/2002JE001927. 1-1.

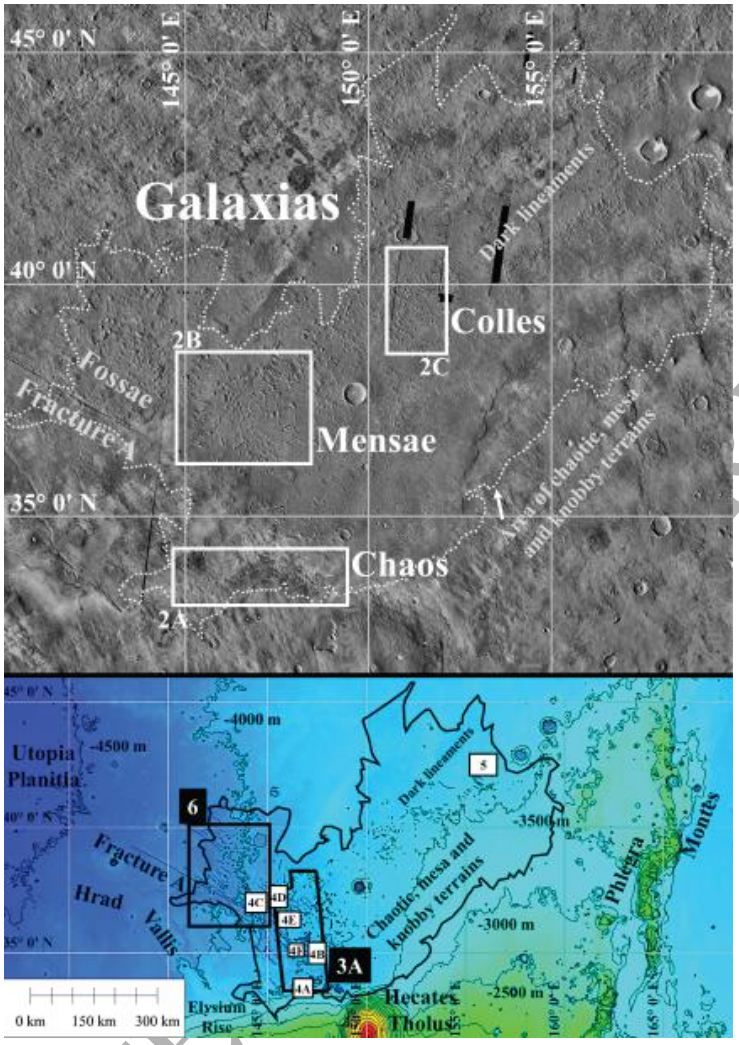

Figure 1 (A) Locations and synoptic overview of the regions Galaxias Chaos, Mensae, Colles and Fossae, including Fracture A (THEMIS DT IR Controlled Mosaic Cebrenia 30N 120E 100 mpp). The dotted line represents the extent of chaotic terrain and mesa-knobby terrains mapped from the GIS. The locations of Figs 2A, 2B and 2C are shown as white boxes. The region characterised by dark lineaments is labelled. (B). Location of Galaxias Chaos, Galaxias Mensae and Galaxias Colles in relation to Hecates Tholus, Hrad Vallis, Utopia Planitia and Phlegra Montes (THEMIS Day IR Controlled Mosaic Cebrenia 30N 120E 100 mpp with MOLA MEGDR 128 ppd color-shaded relief overlay, contours shown at 500 m intervals). Heavy black line bounding

the cross-hatched area shows the extent of chaotic, mesa and knobby terrains (dotted white line in 1A). Line-work within this area shows locations of fractures, pitted cones and broad ridges; numbered boxes show the locations of Figs 3A, 4A-F, 5 and 6, in which these landforms are shown in greater detail. The region characterised by dark lineaments extends southwest from the box showing the location of Fig. 5.

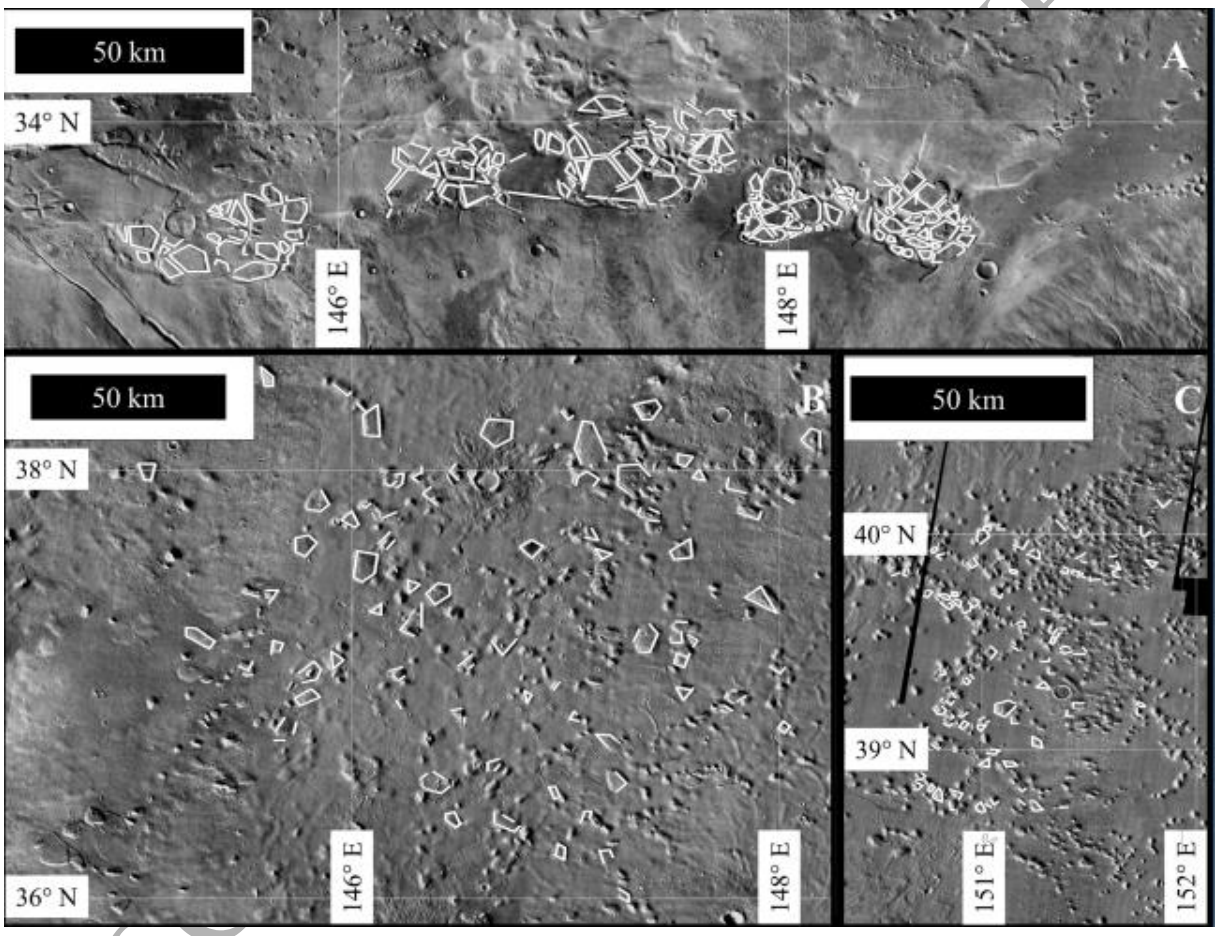

Figure 2. THEMIS Day IR Controlled Mosaic Cebrenia 30N 120E 100 mpp image sub-scenes showing chaotic block and mesa edges digitised for directional analysis. Galaxias Chaos: panel A. Galaxias Mensae: panel B. Galaxias Colles: panel C.

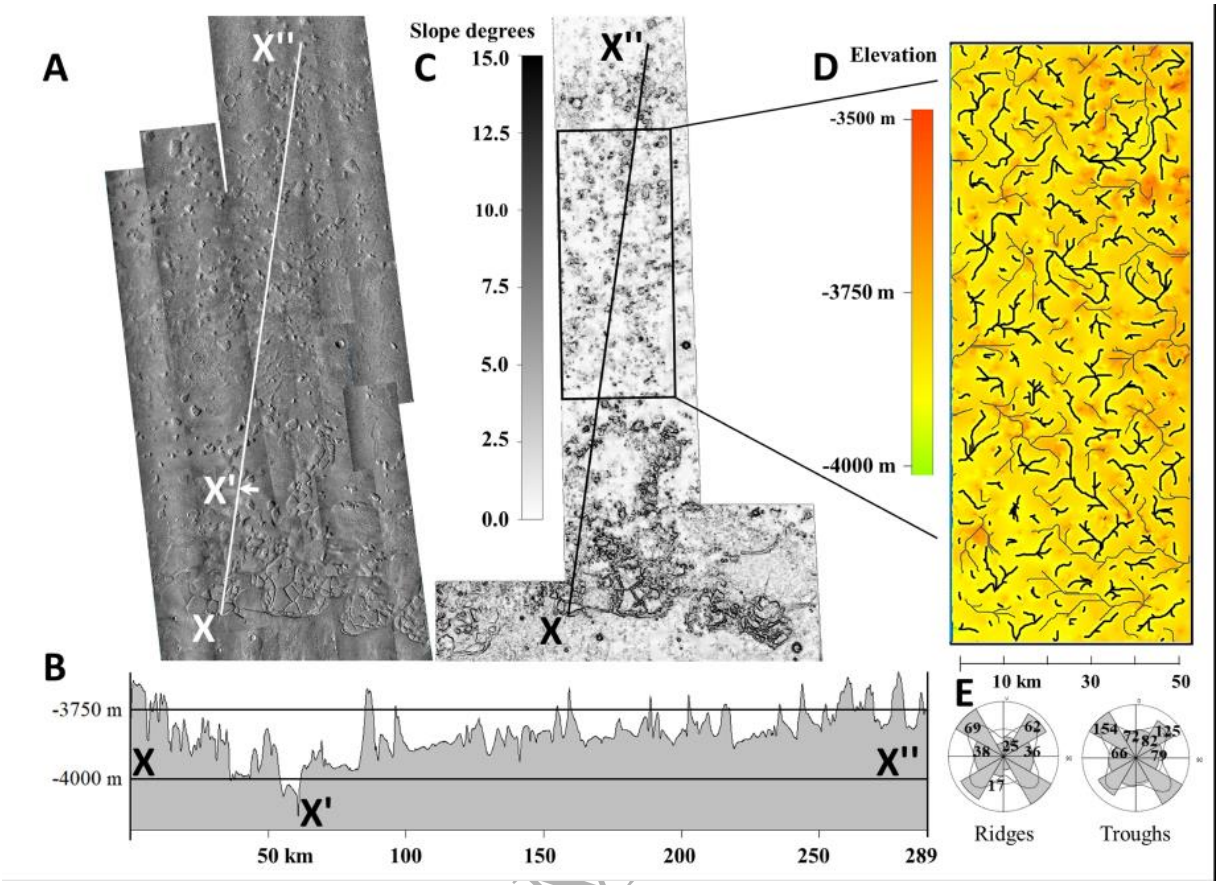

Figure 3 (A).CTX synoptic image mosaic showing relative locations and planimetric morphological attributes of Galaxias Chaos and Galaxias Mensae. The white line shows the path of elevation profile X – X'' (panel B). (B) HRSC elevation profile X - X'', drawn orthogonal to the strike of the regional fractures. The elevation profile reveals the accordance in maximum elevation and uniform thickness of the chaotic plateaus and mesas (typically ~200 m, rarely ~250 m). The inter-mesas are topographically subdued but appear to have oscillatory relief, giving the impression that vertically truncated mesas could occupy the inter-mesas. The profile also shows the Galaxias Fossae valley-form in cross-section (location X'), separating Galaxias Chaos and Galaxias Mensae. (C) Slope steepness map (HRSC 50 m DTM h1284_0000.da4.53) showing relief variability in the inter-mesas. (D) Directional arrangements of mesa assemblages

and inter-assemblage corridors, modelled from the HRSC DTM. (E) Rose diagrams showing directional distributions of the mesa assemblages and inter-assemblage corridors.

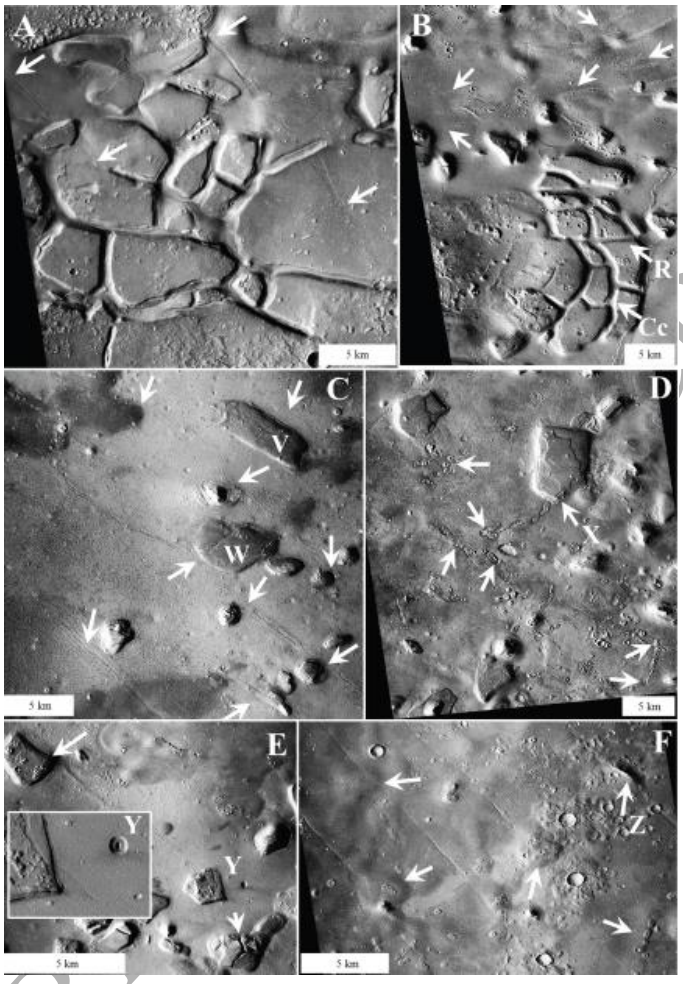

Figure 4 (A) Galaxias Chaos; chaotic terrain and SE-NW fractures (arrowed) (from CTX image B22_018260_2159_XN_35N213W). (B) Mesa assemblage with radial-concentric fractures (examples arrowed and labelled *R*/*Cc*) and adjacent pitted cone chains (arrowed), convergent towards the head of Galaxias Fossae (from CTX image B05_011746_2156_XI_35N212W). (C) Galaxias Mensae; the parallel arrangement of SE_NW fractures is mirrored by the arrangement of free-standing mesas; arrowed mesa edges are located alongside SE-NW fractures; cross-cutting (SW-NE) fractures pervade mesas at V and W (from CTX image

B17_016335_2187_XN_38N215W). (D) Galaxias Mensae; pitted cone chains with bilateral and orthogonal SE-NW/SW-NE arrangements associated with the regional cross-cutting fracture sets; where a pitted cone chain terminates at a mesa, a fracture pervades the mesa directly along strike from the cone chain arrowed at X) (from CTX image B22_018260_2159_XN_35N213W). (E) Galaxias Mensae; a mesa edge directly constrained by an adjacent fracture (arrowed upper left corner of image) contrasts with a mesa (at Y) that is fractured along a strike offset from the fracture in the substrate; indicative of partial rotation of the mesa at Y, perhaps as a consequence of ground disturbance; a deeply pitted crater near Y is indicative of voids in the subsurface, perhaps contributory to local ground disturbance (from CTX image B22_018260_2159_XN_35N213W). (F) Galaxias Mensae, SE-NW fractures have a regular lateral spacing and pitted cones chains (> 2 cones in sequence; examples arrowed) are generally aligned parallel or orthogonal to the SE-NW fractures. Degraded mesas are apparent (example at Z) but rounded hummocks appear to be degraded mesas; SE-NW fractures (example arrowed, top left of panel, ~2 km south of prominent crater) and short chains of pitted cones pervade the hummocks (from CTX image P17_007751_2150_XN_35N214W).

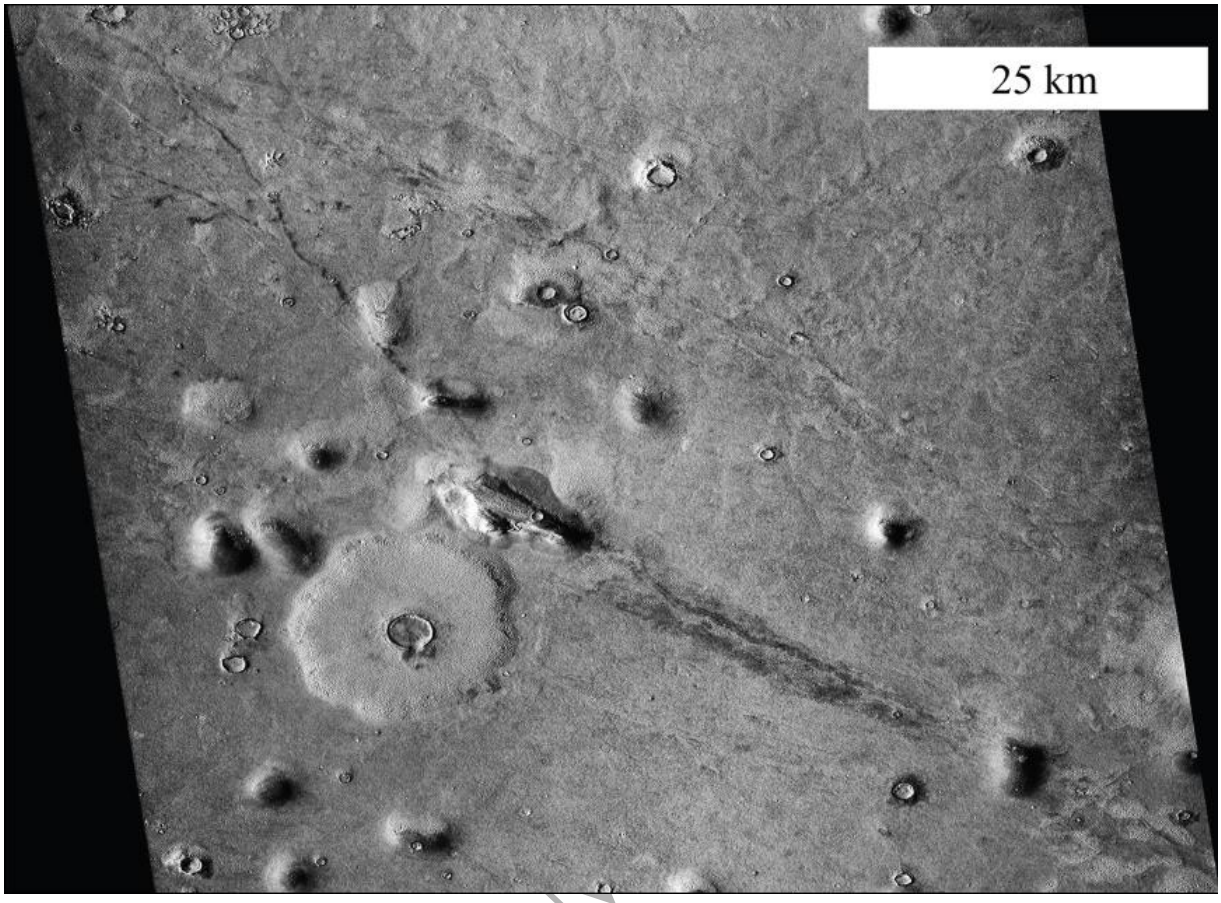

Figure 5. Example of a dark lineament in Galaxias Colles showing the node-like arrangement of mesa and knobs along the feature (part of CTX B21_017640_2227_XN_42N204W).

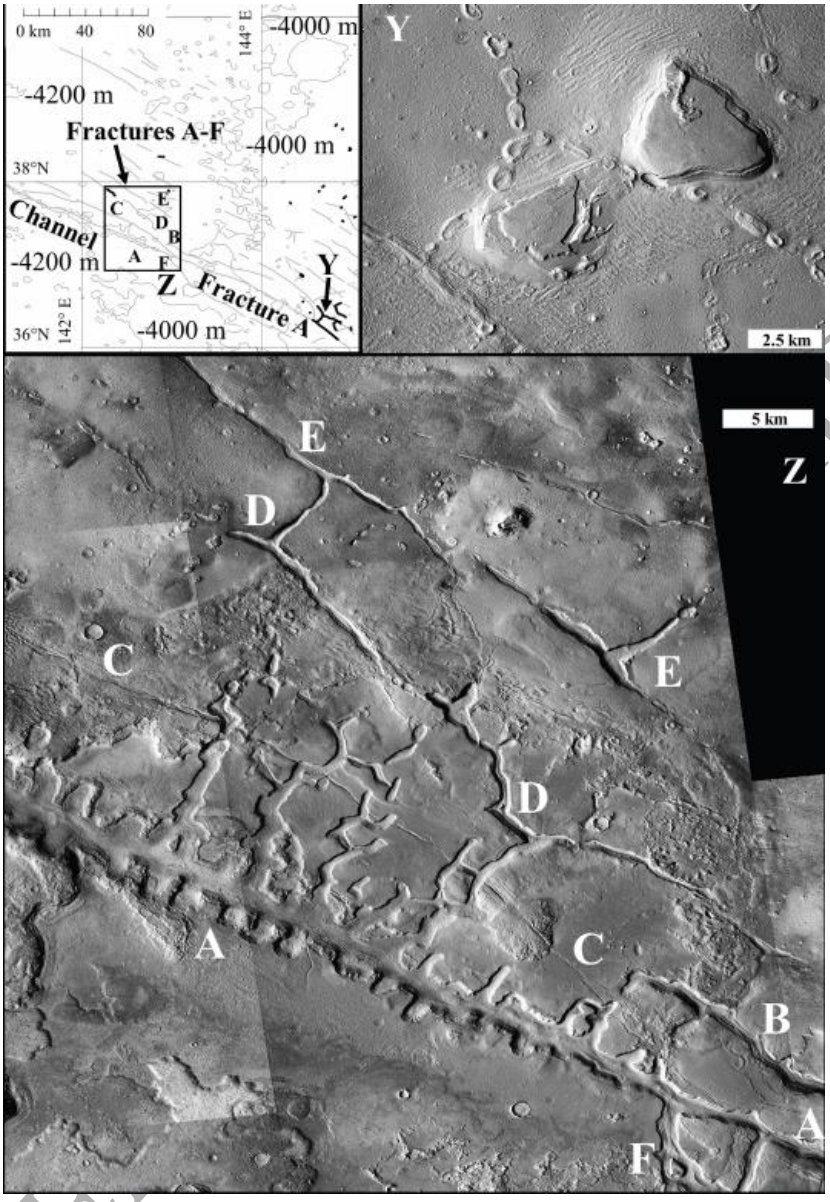

Figure 6. Upper panel (map); spatial and topographic context of primary fractures (grey lines) in Galaxias Fossae, including Fracture A and associated fractures B-F. Inset image Y: pitted cone chains and overlying mesas developed in the upper reaches of Fracture A. The pitted cones compartment the mesas and converge step-wise towards Fracture A by developing curving transitions from primary (SE-NW) to secondary (SW-NE) strike. Erosion of overlying mesas reveals variably-mantled pitted cones; cone-tops are visible as pits where mesas have been

thinned, rather than completely eroded (Part of CTX B21_017680_2179_XN_37N215W). Image panel Z: Fractures A-F, detail showing the trellis pattern (orthogonal) dissection of terrain and consequent chasm-channel network development between fractures A-E (parts of CTX B19_017179_2177_XN_37N217W, P18_008173_2195_XN_39N217W and F20_043565_2156_XN_35N217W).

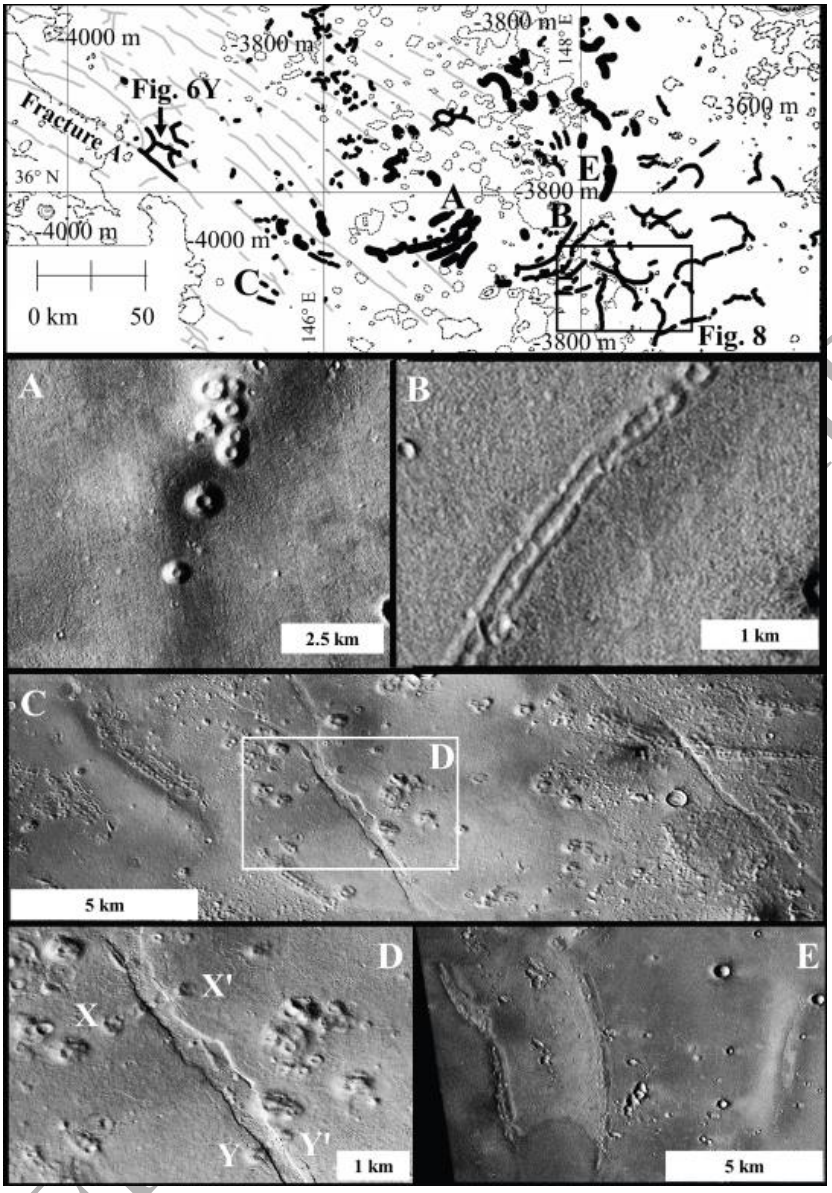

Figure 7. Upper panel (map); spatial arrangement and topographic context of pitted cone chains and broad ridges in Galaxias Mensae. Panel A (from CTX image P16_007395_2148_XN_34N213W): detail of broad ridge with nodal swellings and clusters of pitted cones. Inset panel B (from CTX image B05_011746_2156_XI_35N212W): broad ridges breached by summital chains of pitted cones. Panel C (from CTX image P15_006749_2149_XN_34N214W): broad ridge with flanking, parallel chains of pitted cones

(left edge of image) and pitted cone chains crossing primary fractures (upper right corner and Box D). Panel D: detail of Box D, showing cone chains fractured and displaced into primary fracture. Panel E (from CTX image B18_016625_2179_XN_37N212W): three broad ridges (N-S) showing variable emergence of summital pitted cones. Eastern ridge, no cones evident but summital thinning is apparent. Central ridge is fractured along its summit. Western ridge, summital sequence of pitted cones fully emerged – the ridge is partially onlapped from the west by a darker cap of softened terrain (see text and Fig. 8).

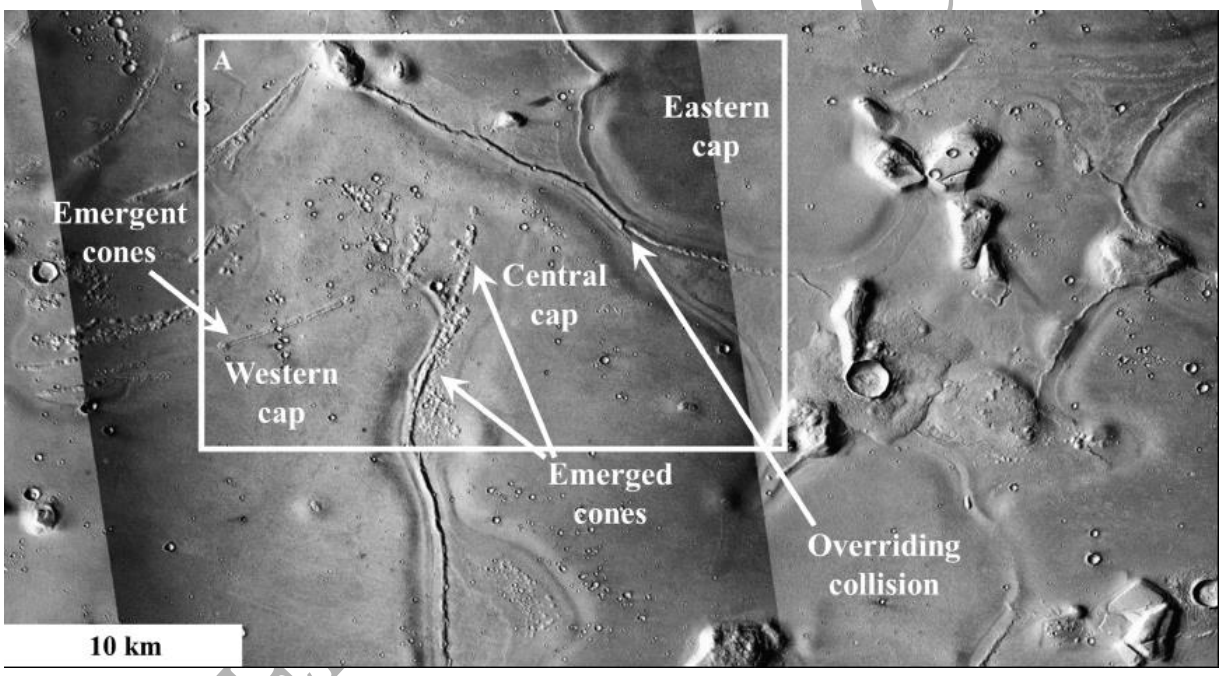

Figure 8. Galaxias Mensae, remnant mesas amid texturally softened terrain caps, lacking angular, polygonal forms; the edges of several mesas are directly bounded by softened terrain caps (CTX B05_011746_2156_XI_35N212W, P17_007685_2133_XN_33N211W and B19_017192_2164_XI_36N211W). Box A: note convergence of softened caps and marginal overriding of central cap onto eastern. Also note that the central cap is overlain by a higher, western cap. Where only the central cap is in place, chains of pitted cones have emerged fully

(arrowed). Where the western cap is in place over the central, pitted cones are only partially emergent (i.e. cone flanks are not revealed).

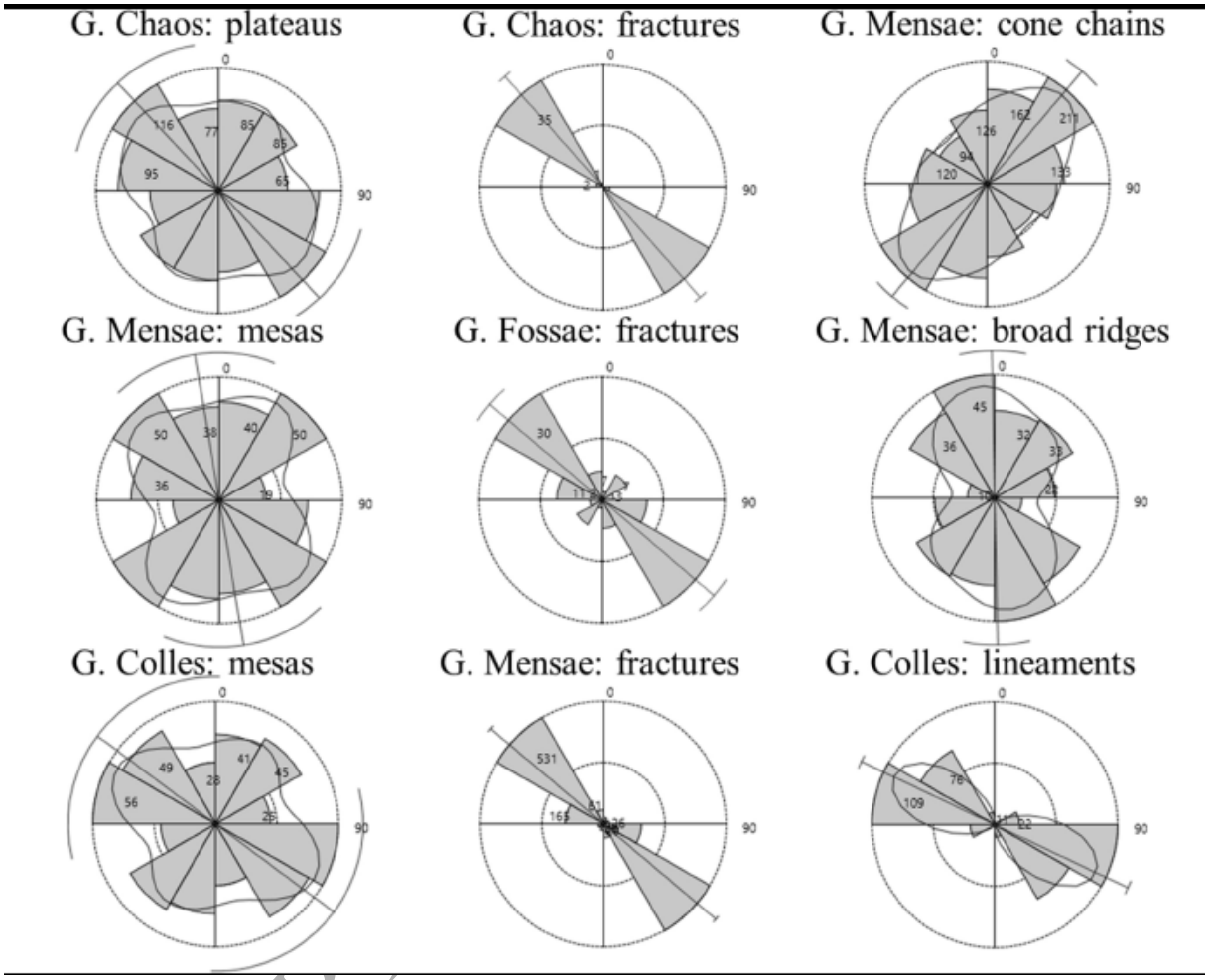

Figure 9. Left stack; Chaos plateau and mesa edge axial orientation planes. Centre stack; primary fracture axial strike planes. Right stack; pitted cone chain, broad ridge and dark lineament axial orientation planes. External arcs are the bootstrapped 95% confidence interval. The circular kernel density estimate is shown as a black outline within the circles (not required for the fracture strike distributions, which are tightly unimodal.

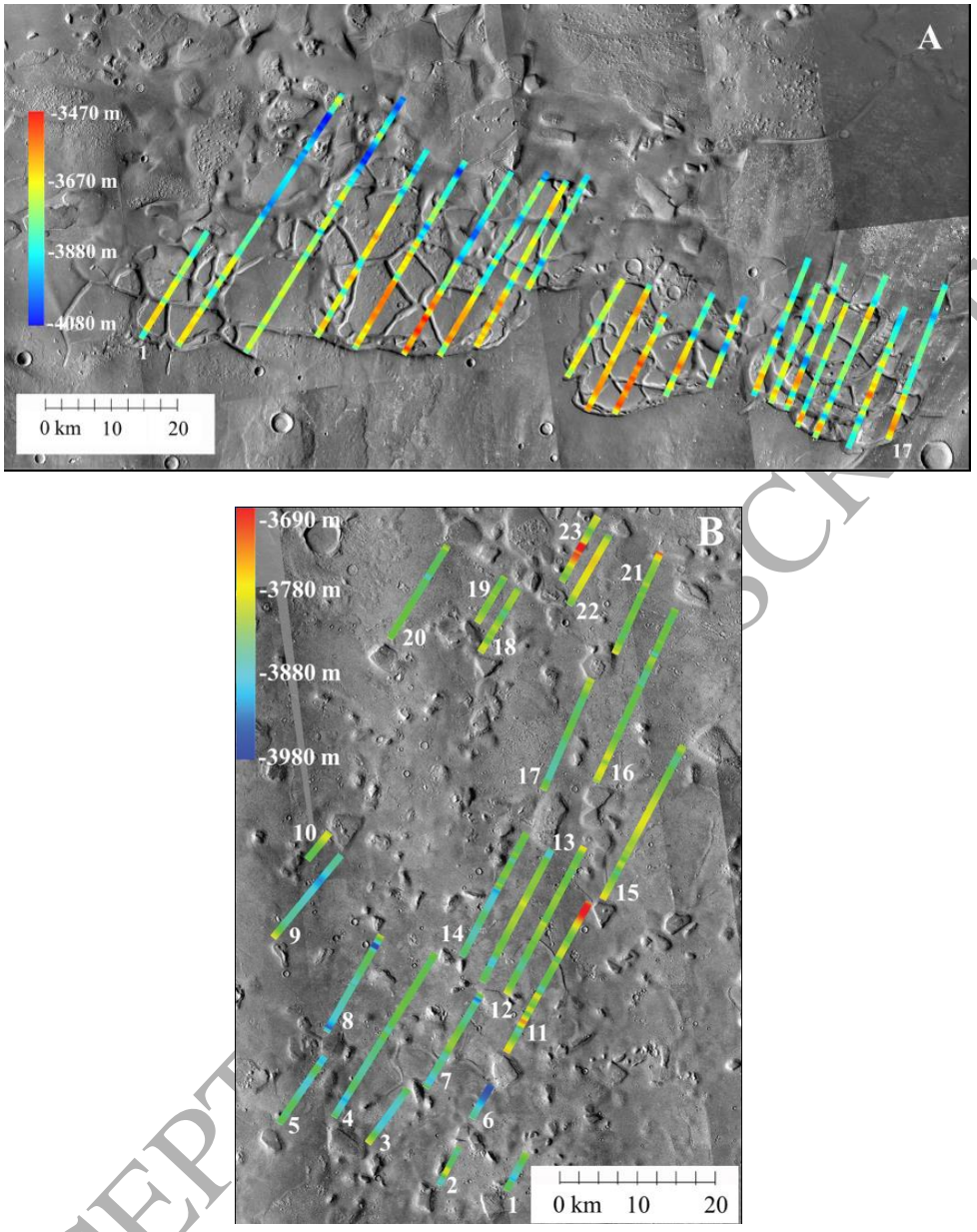

Figure 10. (A) Relief of Galaxias Chaos plateau-fracture transition, plotted as colour-shaded strips showing elevation variation orthogonal to the dominant SE-NW fractures in the region (HRSC elevation data over CTX mosaic). (B) Inter-mesa relief in Galaxias Mensae plotted as colour-shaded strips showing elevation variation orthogonal to the SE-NW fractures in the region (HRSC elevation data over CTX mosaic).

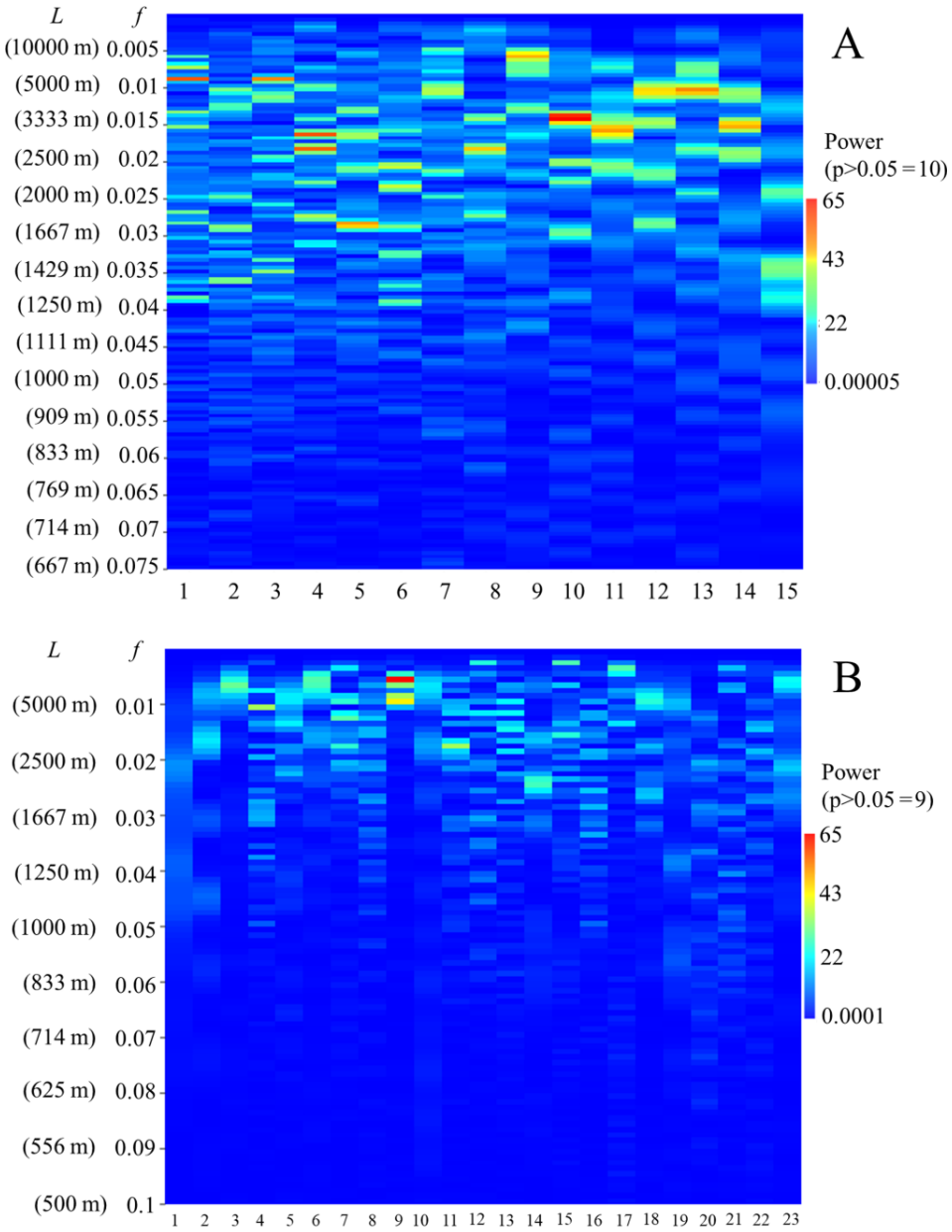

Figure 11 Matrix plots of the power spectral density of the d = 1 elevation series derived from the elevation profiles in Fig 10: (A) Galaxias Chaos, plateau-trough oscillations; (B) Galaxias Mensae, inter-mesa terrain oscillations. The plots show the frequency peaks (and associated wavelengths, or spatial interval, *L*) of each d = 1 elevation series; non-random frequency peaks

exceed the stated critical probability level, p(<0.05). The dominant scale (L_{dom}) over which relief oscillates (i.e. dominant scale of spatial cyclicity) along each detrended series is given by $L_{dom} = (1/lag)f_{peak}$, where the lag = 50 m (the along-profile sampling interval) and f_{peak} is the frequency with the maximum power. Statistical tests were carried using the median values of L_{dom} from each region: Galaxias Chaos, plateau-trough oscillations in elevation; Galaxias Mensae, inter-mesa terrain oscillations in elevation.

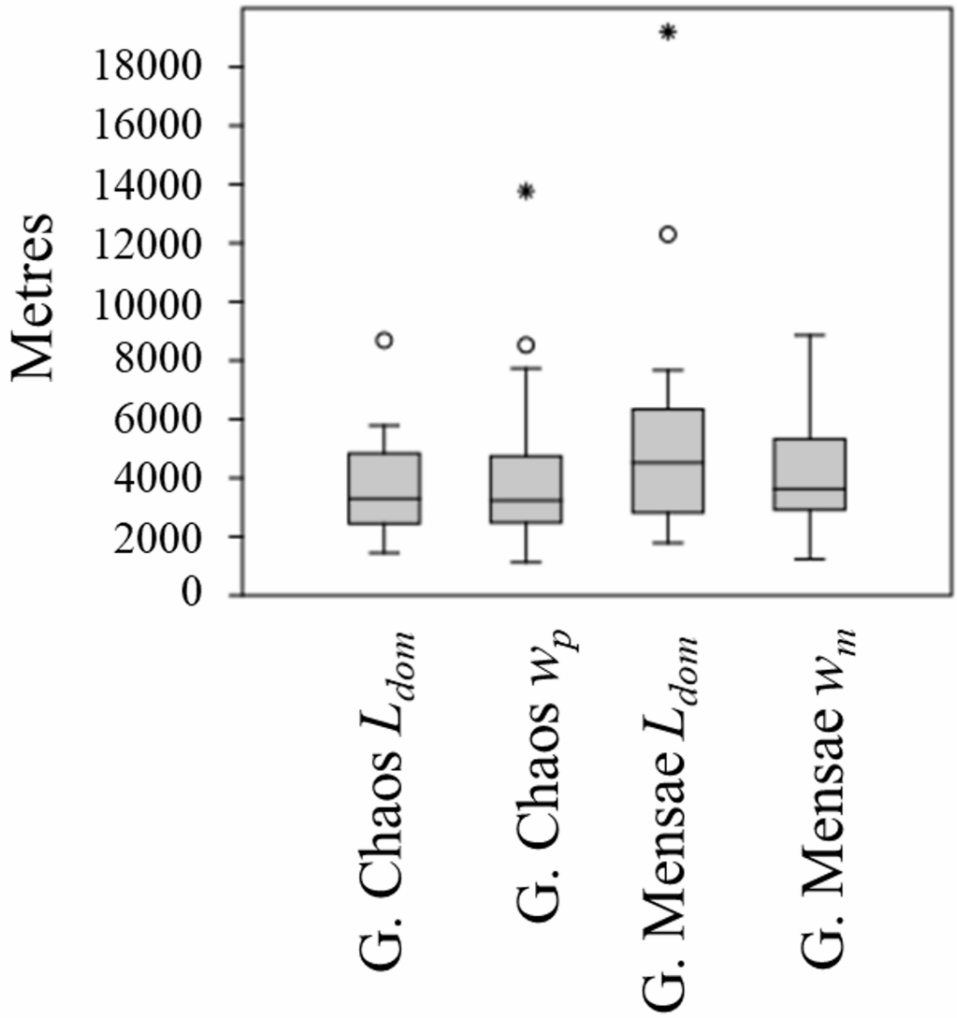

Figure 12. Box and whisker plot of the medians, inter-quartile range and outliers of L_{dom} (dominant spatial scale of relief cyclicity, chaotic terrain, Galaxias Chaos), L_{dom} (dominant spatial scale of relief cyclicity, inter-mesa terrain, Galaxias Mensae), w_p (plateau maximum width, Galaxias Chaos) and w_m (mesa maximum width, Galaxias Mensae). There is no significant difference between the medians.